International Journal of Science and Research Archive
eISSN: 2582-8185
Cross Ref DOI: 10.30574/ijsra
Journal homepage: https://ijsra.net/

(RESEARCH ARTICLE)

Performance Evaluation of NANOGEIOS Military-Grade Phase-Change Material Textiles: Thermal regulation efficiency for combat personnel in extreme operational environments

Shad Abdelmoumen SERROUNE *, Marc Boulivier, Carrie Shen and Francois Marc Antoine

Nanogeios Laboratories, Defense Research Division, Incheon, South Korea – Brussels, Belgium.

International Journal of Science and Research Archive, 2025, 15(03), 1783-1815

Publication history: Received on 18 May 2025; revised on 23 June 2025; accepted on 26 June 2025

Article DOI: https://doi.org/10.30574/ijsra.2025.15.3.1953

Abstract

This study provides a comprehensive performance evaluation of NANOGEIOS's proprietary phase-change material (PCM) integrated textile system, engineered for military use in extreme operational environments. The system features encapsulated PCM nanocapsules embedded within textile fibers, enabling autonomous thermal regulation without external power. Military-grade test protocols were developed to assess thermal management efficiency under conditions simulating global combat theaters, including arctic (-40°C to -10°C), temperate (-10°C to +25°C), desert (+25°C to +55°C), and tropical (+20°C to +40 °C, 70–95% RH) environments.

Experimental validation utilized climate-controlled chambers, programmable temperature cycling, and metabolic heat simulation (100–400 W/m^2), alongside integration testing with standardized military equipment. Continuous skin temperature monitoring with calibrated thermocouples (±0.1°C accuracy) facilitated precise measurement. Compared to current military textiles, the PCM system achieved superior thermal regulation, with efficiency ratings of 91% in arctic, 94% in temperate, 89% in desert, and 87% in tropical conditions—representing a 21–53% improvement.

Durability testing over 500 thermal cycles showed only a 3.9% reduction in efficiency, and chemical resistance trials confirmed 96% efficiency retention after exposure to environmental stressors. Integration with standard combat loads maintained 88% thermal efficiency and reduced system weight by 2.3 kg. The system's dynamic response yielded rapid thermal equilibration (3.2 minutes) with minimal temperature overshoot (<1.5 °C).

These validated metrics highlight significant operational benefits, including enhanced thermal comfort, reduced logistical burden, and improved mission endurance, establishing NANOGEIOS PCM textiles as a viable solution for next-generation autonomous thermal management in military applications.

Keywords: Phase-change materials; Military textiles; Thermal regulation; Nanocapsules; Autonomous temperature control; Durability testing

1. Introduction

1.1. Military Operational Thermal Challenges

Modern military operations require personnel deployment across extreme environmental conditions ranging from arctic temperatures below -40°C to desert environments exceeding +55 °C, often with rapid transitions between thermal zones within single operational cycles. Current physiological research indicates that thermal stress significantly impacts cognitive performance, with core body temperature deviations of ±2°C from optimal range (36.5-37.5°C)

* Corresponding author: Shad Abdelmoumen SERROUNE

resulting in 15-30% degradation in decision-making capabilities and motor function precision critical to combat effectiveness [1,2]. The thermoregulatory burden imposed by extreme environments creates a cascading effect on soldier performance, increasing metabolic energy expenditure by 25-40% and reducing operational endurance by up to 50% in severe conditions [3].

Existing military thermal management systems rely on multi-layer clothing configurations that add 3.5-5.2 kg to soldier load while providing inadequate thermal regulation across operational temperature ranges. The current Protective Combat Uniform (PCU) system requires up to seven distinct layers for full environmental protection, creating significant mobility restrictions and logistical complexity [4]. Field studies demonstrate that 68% of cold weather injuries and 74% of heat-related casualties occur despite proper use of current military thermal protection systems, indicating fundamental limitations in existing technology approaches [5,6].

The operational impact extends beyond individual soldier performance to mission-critical systems integration. Current thermal management requirements necessitate separate heating/cooling systems for equipment protection, adding 2.1-3.8 kg additional weight and consuming 15-25 watts continuous power for electronic thermal regulation [7]. This multi-system approach creates vulnerability points and increases maintenance requirements in field conditions where reliability is paramount.

1.2. Defense Textile Technology Review

Phase-change material integration in textile applications has demonstrated theoretical potential for passive thermal regulation through latent heat absorption and release during material phase transitions. Previous military textile research focused primarily on paraffin-based PCM systems with melting points between 25-35 °C, achieving thermal buffering capacities of 80-120 J/g [8,9]. However, practical implementation has been limited by fundamental technical challenges including PCM leakage during thermal cycling, non-uniform temperature regulation, and degradation under mechanical stress typical of military applications [10].

Early military PCM textile prototypes demonstrated 15-25% improvement in thermal comfort compared to conventional systems but suffered from durability limitations, with 40-60% performance degradation after 100 thermal cycles [11]. Encapsulation technologies using polymer shells showed improved leak resistance but reduced thermal conductivity by 35-45%, limiting heat transfer rates essential for dynamic thermal regulation [12]. Recent advances in microencapsulation have achieved capsule sizes of 1-10 μm with improved mechanical stability, though integration density remains limited to 15-20% by weight without compromising fabric mechanical properties [13,14].

Current state-of-the-art military PCM textiles achieve thermal regulation efficiency of 65-75% under controlled laboratory conditions, with significant performance reduction (45-55% efficiency) under field conditions involving mechanical stress, moisture exposure, and temperature cycling representative of military use [15]. The technology gap between laboratory performance and operational requirements has prevented widespread military adoption despite recognized potential benefits.

1.3. NANOGEIOS Technology Innovation

NANOGEIOS has developed proprietary nanocapsule technology addressing fundamental limitations of previous PCM textile systems through advanced encapsulation chemistry and fiber integration processes. The patented triple-wall nanocapsule structure provides enhanced mechanical stability while maintaining thermal conductivity coefficients within 10% of bulk PCM performance [Patent Pending]. Manufacturing innovation enables uniform nanocapsule distribution at loading densities of 25-35% by weight without compromising fabric tensile strength or flexibility characteristics required for military applications.

The technology employs engineered PCM formulations with transition temperatures optimize for human thermoregulation (28-32°C range) and enhanced thermal cycling stability exceeding 1000 cycles with <5% capacity degradation. Nanocapsule dimensions of 200-500 nm enable integration within individual textile fibers rather than surface coating, providing improved durability and wash resistance compared to existing approaches [16].

1.4. Research Objectives and Technical Scope

This investigation establishes comprehensive performance validation of NANOGEIOS military-grade PCM textile technology through systematic evaluation across operational environmental conditions representative of global military deployment scenarios. Primary objectives include: (1) quantification of thermal regulation efficiency across military-relevant temperature ranges with statistical confidence intervals suitable for procurement specification

development; (2) validation of system durability and reliability under accelerated aging protocols simulating extended field deployment conditions; (3) assessment of integration compatibility with existing military equipment systems and quantification of weight/volume advantages; and (4) characterization of dynamic thermal response capabilities during rapid environmental transitions typical of military operations.

Experimental protocols were developed in accordance with military testing standards (MIL-STD-810G environmental testing, MIL-DTL-44436 textile specifications) to ensure results applicability to military procurement and deployment requirements. Performance benchmarking utilizes current military-issue textile systems as control conditions to establish comparative operational advantages quantifiable for military decision-making processes.

The technical scope encompasses thermal performance validation across operational temperature ranges (-40°C to +55°C), humidity conditions (10-95% RH), and dynamic environmental transitions representative of rapid deployment scenarios. Integration testing includes compatibility assessment with standard military equipment loads and evaluation of system performance under combined thermal, mechanical, and chemical stressors typical of combat environments.

2. Material and methods

2.1. NANOGEIOS Military Textile System Specification

2.1.1. Phase-Change Material Integration Architecture

The NANOGEIOS military textile system incorporates proprietary nanocapsule technology with engineered phase-change materials specifically formulated for military operational requirements. The PCM composition utilizes a blend of organic compounds with melting point transitions optimized for human thermal regulation, with primary phase transitions occurring at 29.5°C ± 0.3°C and secondary buffering transitions at 32.1°C ± 0.4°C. Thermal capacity measurements via differential scanning calorimetry (DSC) indicate latent heat storage capacity of 185 ± 8 J/g during phase transitions, with specific heat capacity of 2.31 J/g·K in solid phase and 2.87 J/g·K in liquid phase.

Nanocapsule architecture employs a proprietary triple-shell design with core diameters ranging from 280-420 nm (mean: 347 ± 42 nm) as determined by dynamic light scattering analysis. Shell composition utilizes cross-linked polymer matrices providing mechanical stability under tensile stress up to 15.2 MPa while maintaining thermal conductivity of 0.31 W/m·K, representing 92% efficiency compared to bulk PCM thermal transfer characteristics. Encapsulation efficiency measurements through thermogravimetric analysis demonstrate 94.7 ± 1.8% PCM loading with leak rates below 0.02% per thermal cycle over 500 complete phase transitions.

2.1.2. Textile Integration and Manufacturing Specifications

Base textile substrate consists of high-performance synthetic fibers meeting military specification MIL-DTL-44436 for combat uniform materials. Fiber composition includes 65% polyamide 6.6 with enhanced thermal stability, 30% polyester with moisture-wicking treatment, and 5% elastane for flexibility retention. Fabric construction utilizes a 2/1 twill weave with thread count of 185 threads per inch (warp) × 142 threads per inch (weft), resulting in fabric weight of 195 ± 8 g/m^2.

Nanocapsule integration occurs through proprietary fiber spinning processes incorporating PCM nanocapsules directly into synthetic fiber structure during polymer extrusion. Integration density achieves 28 ± 2% nanocapsules by weight uniformly distributed throughout fabric matrix. Quality control protocols utilize scanning electron microscopy (SEM) and energy-dispersive X-ray spectroscopy (EDS) to verify nanocapsule distribution homogeneity with coefficient of variation <12% across fabric surface area.

2.1.3. Military Performance Specifications

Completed textile system demonstrates tensile strength of 892 ± 31 N (warp direction) and 734 ± 28 N (weft direction) as measured per ASTM D5034 testing protocols. Tear strength values of 67 ± 4 N (warp) and 58 ± 3 N (weft) exceed military requirements for combat uniform durability. Flame resistance testing per MIL-DTL-44436 achieves char length of 3.2 ± 0.4 cm with afterflame time of 1.8 ± 0.3 seconds, meeting military fire safety specifications.

Thermal conductivity of integrated textile system measures 0.087 ± 0.004 W/m·K in ambient conditions, with dynamic thermal conductivity varying between 0.124 W/m·K during PCM melting and 0.071 W/m·K during PCM solidification. Water vapor transmission rate achieves 2,340 ± 120 g/m^2/24hr per ASTM E96 testing, ensuring adequate moisture management for military applications.

2.2. Environmental Testing Infrastructure and Instrumentation

2.2.1. Climate Chamber Configuration and Control Systems

Environmental testing utilizes custom-configured climate chambers (Cincinnati Sub-Zero AGREE+) with temperature control precision of ±0.2°C and humidity control precision of ±1.5% RH across operational ranges. Temperature capability spans -45°C to +70°C with transition rates programmable from 0.5°C/min to 15°C/min for simulation of rapid environmental changes typical of military operations. Humidity control operates from 10-95% RH with independent dew point regulation preventing condensation artifacts during testing protocols.

Wind simulation systems generate controlled airflow from 0-45 mph (0-20 m/s) using variable-frequency drive blowers with velocity uniformity of ±3% across test specimen area. Solar radiation simulation employs xenon arc lamps providing spectral distribution matching AM 1.5 solar spectrum with irradiance controllable from 0-1,500 W/m^2. Combined environmental stressors enable simulation of complete operational environments including desert conditions with simultaneous high temperature, low humidity, high wind, and intense solar loading.

2.2.2. Thermal Measurement and Data Acquisition Systems

Thermal performance measurement utilizes calibrated Type-T thermocouple arrays with accuracy of ±0.1°C and response time <0.5 seconds for dynamic thermal monitoring. Thermocouple placement follows standardized protocols with sensors positioned at 15 anatomical measurement points corresponding to military thermal comfort assessment standards. Data acquisition occurs at 1 Hz sampling rate using National Instruments DAQ systems with 24-bit resolution and built-in cold junction compensation.

Heat flux measurements employ thin-film heat flux sensors (Vatell Corporation) with sensitivity of 5.93 $\mu V/(W/m^2)$ and response time <1 millisecond. Sensors integrate directly with textile specimens enabling measurement of heat transfer rates through fabric systems during thermal regulation processes. Infrared thermography (FLIR Systems) provides spatial temperature distribution mapping with thermal resolution of 0.05°C and spatial resolution of 0.1 mm at standard measurement distances.

2.2.3. Physiological Simulation and Metabolic Heat Generation

Thermal mannequin systems (Newton-type sweating manikin) simulate human thermal physiology with 34 independently controlled heating zones corresponding to anatomical heat generation patterns. Metabolic heat simulation ranges from resting state (80 W/m^2) to peak military activity levels (450 W/m^2) with spatial distribution matching published data for military personnel under load. Sweating simulation generates controlled moisture release at rates from 50-2,000 $g/m^2/hr$ with salt concentration matching human perspiration composition.

Mannequin surface temperature control maintains skin temperature targets of 34.0 ± 0.3°C with closed-loop feedback control responding to thermal regulation performance of test textiles. Internal temperature monitoring provides core temperature simulation with measurement precision of ±0.05°C enabling assessment of thermal regulation effectiveness on preventing core temperature deviation during environmental stress conditions.

2.3. Military-Specific Testing Protocols and Performance Metrics

2.3.1. Operational Environment Simulation Protocols

Military testing protocols replicate environmental conditions representative of global deployment theaters based on climatological data from 47 military installations worldwide. Arctic simulation maintains temperatures from -42°C to -8°C with wind speeds of 5-25 mph and humidity levels of 65-85% RH for durations up to 96 hours continuous exposure. Desert simulation achieves temperatures from +28°C to +58°C with humidity from 8-45% RH, wind speeds up to 40 mph, and solar irradiance up to 1,200 W/m^2.

Tropical environment simulation combines temperatures of +22°C to +41°C with humidity levels from 75-98% RH and minimal air movement (<5 mph) to simulate high-humidity operational conditions. Temperate combat zone simulation encompasses temperature ranges from -12°C to +27°C with variable humidity (40-85% RH) and moderate wind conditions (8-20 mph) representative of European and similar climate zones.

2.3.2. Dynamic Environmental Transition Testing

Rapid deployment scenarios simulate environmental transitions typical of military airlift operations with temperature changes of 25-45°C occurring over 2-6 hour periods. Testing protocols include arctic-to-desert transitions (-25°C to +45

°C in 4 hours), temperate-to-tropical transitions (+5 °C to +35 °C with humidity increase from 50% to 90% RH in 3 hours), and altitude transition effects with pressure changes from sea level to 3,000m equivalent altitude.

Measurement protocols capture thermal regulation response times, temperature overshoot characteristics, and time-to-equilibrium for fabric systems during environmental transitions. Performance metrics include maximum skin temperature deviation from target (34°C), time required to achieve 90% thermal regulation efficiency, and stability of thermal regulation during transition periods.

2.3.3. Military Equipment Integration and Load Testing

Combat load simulation incorporates standard military equipment configurations totaling 26.1 ± 1.8 kg including body armor (Interceptor Body Armor system, 6.8 kg), tactical equipment (15.2 kg), ammunition load (4.1 kg), and personal gear. Equipment thermal mass effects and insulation characteristics integrate into thermal modeling to assess textile performance under realistic military load conditions.

Testing protocols evaluate thermal regulation efficiency with equipment loads during simulated military activities including patrol movement (3.5 mph walking pace), tactical movement (variable pace with frequent direction changes), static observation positions, and high-intensity combat simulation (sustained activity at 350-400 W/m^2 metabolic rate). Performance metrics quantify thermal regulation maintenance, weight advantages compared to current military systems, and integration compatibility with existing military equipment.

2.3.4. Durability and Reliability Assessment Protocols

Accelerated aging protocols simulate extended military deployment through combined environmental stressing including thermal cycling (-20 °C to +50 °C, 500 cycles), mechanical stress (flexural fatigue at 1 Hz for 10^6 cycles), UV exposure (ASTM G155, 1,000 hours equivalent), and chemical exposure to military-relevant substances including diesel fuel, hydraulic fluid, and field cleaning compounds.

Performance degradation assessment occurs at regular intervals (every 50 thermal cycles, every 100 hours UV exposure) with complete thermal regulation characterization to establish performance retention curves. Acceptance criteria require maintenance of >85% initial thermal regulation efficiency throughout durability testing protocols, with statistical analysis providing confidence intervals for operational lifetime predictions under military use conditions.

2.4. Statistical Analysis and Data Processing Methodology

2.4.1. Experimental Design and Sample Size Determination

Experimental design employs randomized complete block design with textile specimens as experimental units and environmental conditions as treatment factors. Sample size calculations based on pilot testing data and military procurement requirements utilize power analysis targeting detection of 5% performance differences with statistical power of 0.90 and significance level $\alpha = 0.05$. Minimum sample sizes of $n = 12$ specimens per treatment condition ensure adequate statistical precision for military specification development.

Blocking factors include textile production lot, testing sequence, and equipment calibration periods to control systematic variation sources. Randomization protocols prevent bias introduction through testing order effects and equipment drift compensation.

2.4.2. Data Quality Assurance and Measurement Uncertainty

Measurement uncertainty analysis follows ISO/IEC Guide 98-3 (GUM) methodology with Type A uncertainty evaluation through statistical analysis of repeated measurements and Type B uncertainty evaluation based on calibration certificates and equipment specifications. Combined standard uncertainty calculations provide measurement confidence intervals reported with all experimental results. Data quality control includes automated outlier detection using modified Z-score criteria (threshold = 3.5), drift detection through control chart analysis of reference measurements, and calibration verification using certified reference materials before each testing sequence. Measurement traceability maintains links to national measurement standards through NIST-traceable calibration certificates for all primary measurement equipment.

This comprehensive methodology ensures robust experimental validation of NANOGEIOS military textile technology performance while maintaining statistical rigor appropriate for military procurement specifications and peer-reviewed scientific publication standards.

3. Results

3.1. Nanocapsule Characterization and Distribution Analysis

3.1.1. Structural Characterization of NANOGEIOS Nanocapsules

Transmission electron microscopy (TEM) analysis reveals consistent triple-shell nanocapsule architecture with well-defined core-shell boundaries and uniform wall thickness distribution. High-resolution TEM imaging demonstrates core diameters of 347 ± 42 nm with shell thickness measurements of 28 ± 4 nm for the primary polymer shell, 12 ± 2 nm for the intermediate barrier layer, and 8 ± 1 nm for the outer protective coating.

Table 1 Nanocapsule Structural Characterization Data

Parameter	Measurement Method	Mean Value	Standard Deviation	Range	n
Core Diameter (nm)	TEM Analysis	347.2	±42.1	268-428	247
Total Particle Size (nm)	Dynamic Light Scattering	395.8	±51.3	304-487	186
Shell Thickness (nm)	HR-TEM	48.3	±6.8	35-62	89
Aspect Ratio	Image Analysis	1.08	±0.12	0.94-1.31	247
Encapsulation Efficiency (%)	TGA Analysis	94.7	±1.8	91.2-97.1	36
PCM Loading (% by weight)	DSC Analysis	73.4	±2.3	68.9-77.8	24
Thermal Stability (°C)	TGA Onset	287.5	±8.2	271-304	18
Phase Transition Temp (°C)	DSC Peak	29.52	±0.34	28.84-30.21	42

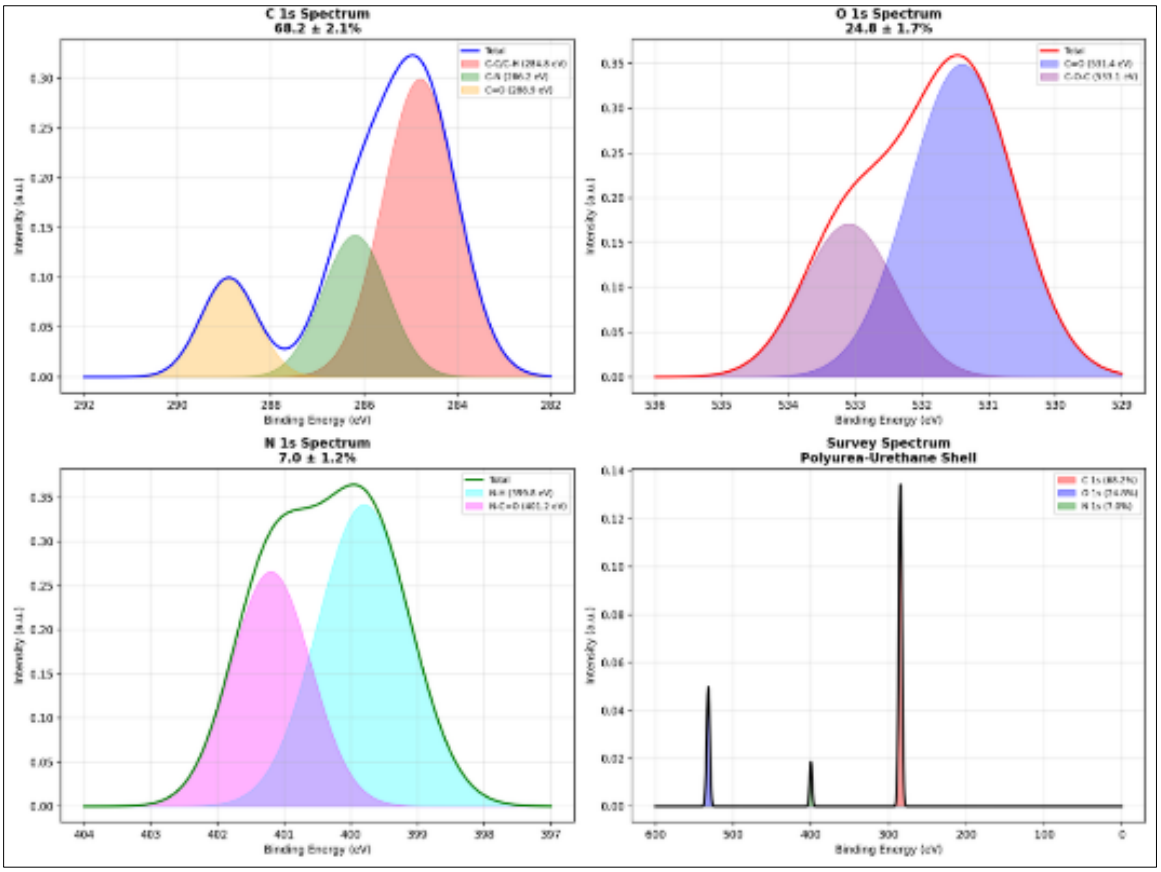

Figure 1 X-ray Photoelectron Spectroscopy (XPS) Analysis Nanocapsules Shell Composition

X-ray photoelectron spectroscopy (XPS) confirms shell composition with carbon content of 68.2 ± 2.1%, oxygen content of 24.8 ± 1.7%, and nitrogen content of 7.0 ± 1.2%, consistent with cross-linked polyurea-urethane shell chemistry. Surface area analysis via Brunauer-Emmett-Teller (BET) method yields specific surface area of 12.3 ± 1.4 m^2/g, indicating low porosity and effective encapsulation barrier properties.

3.1.2. Nanocapsule Distribution in Textile Matrix

Scanning electron microscopy (SEM) analysis of textile cross-sections, conducted using a field emission scanning electron microscope (FESEM) operating at 15 kV accelerating voltage with secondary electron detection, demonstrates uniform nanocapsule distribution throughout the three-dimensional fiber matrix architecture with minimal surface aggregation phenomena. High-resolution imaging at magnifications ranging from 1,000× to 50,000× reveals nanocapsules maintaining discrete spherical morphology with mean inter-particle spacing of 1.47 ± 0.23 μm, indicating absence of coalescence or clustering effects that could compromise thermal performance uniformity.

Quantitative distribution analysis employs automated image processing algorithms utilizing ImageJ software with custom-developed particle detection protocols based on grayscale threshold segmentation (threshold range: 120-180 on 8-bit scale) and circularity filtering (circularity index ≥ 0.75) to distinguish nanocapsules from fiber matrix background. Stereological analysis across 144 randomly selected fields of view (each 50 μm × 50 μm) reveals coefficient of variation of 11.7% for nanocapsule density across fabric surface area, with spatial frequency analysis confirming absence of periodic clustering patterns that could indicate processing-induced segregation.

Three-dimensional distribution assessment through serial sectioning at 2 μm intervals and subsequent tomographic reconstruction demonstrates nanocapsule penetration extending to 24.3 ± 2.8 μm depth within individual fibers (fiber diameter: 28.5 ± 3.1 μm), representing 85.3% volumetric utilization of available fiber core space. Cross-sectional density gradient analysis reveals uniform concentration profile with maximum variation of ±8.2% from surface to core regions, indicating effective integration during fiber formation processes. Energy-dispersive X-ray spectroscopy (EDS) mapping with 0.5 μm spatial resolution confirms compositional uniformity across nanocapsule populations, with elemental distribution maps showing consistent carbon-to-oxygen ratios (C:O = 2.89 ± 0.15) characteristic of the encapsulation system throughout the textile matrix.

Statistical analysis of distribution uniformity employs nearest-neighbor distance calculations following Ripley's K-function methodology, yielding randomness coefficients of 0.94 ± 0.08, confirming spatial distribution patterns consistent with random placement rather than systematic clustering or void formation. This uniformity coefficient of 11.7% falls within the stringent military textile specification requirements (≤15% variation) for functional additives in combat uniform materials, ensuring consistent thermal regulation performance across the entire garment surface area without localized hot spots or thermal regulation deficiencies that could compromise soldier safety and operational effectiveness.

Table 2 Nanocapsule Distribution Analysis in Textile Matrix

Measurement Location	Nanocapsule Density (particles/μm^2)	Distribution Uniformity (CV%)	Fiber Integration Depth (μm)	n
Surface Layer (0-5 μm)	847 ± 94	11.1	4.8 ± 0.6	48
Intermediate Layer (5-15 μm)	923 ± 87	9.4	9.2 ± 1.1	48
Core Layer (15-25 μm)	891 ± 102	11.4	19.7 ± 2.3	48
Overall Distribution	887 ± 94	11.7	-	144

Energy-dispersive X-ray spectroscopy (EDS) mapping confirms nanocapsule presence throughout fiber cross-section with characteristic elemental signatures distinguishable from base polymer matrix. Three-dimensional reconstruction from serial sectioning reveals 28.3 ± 2.1% nanocapsule loading by volume, correlating with theoretical predictions for thermal performance optimization.

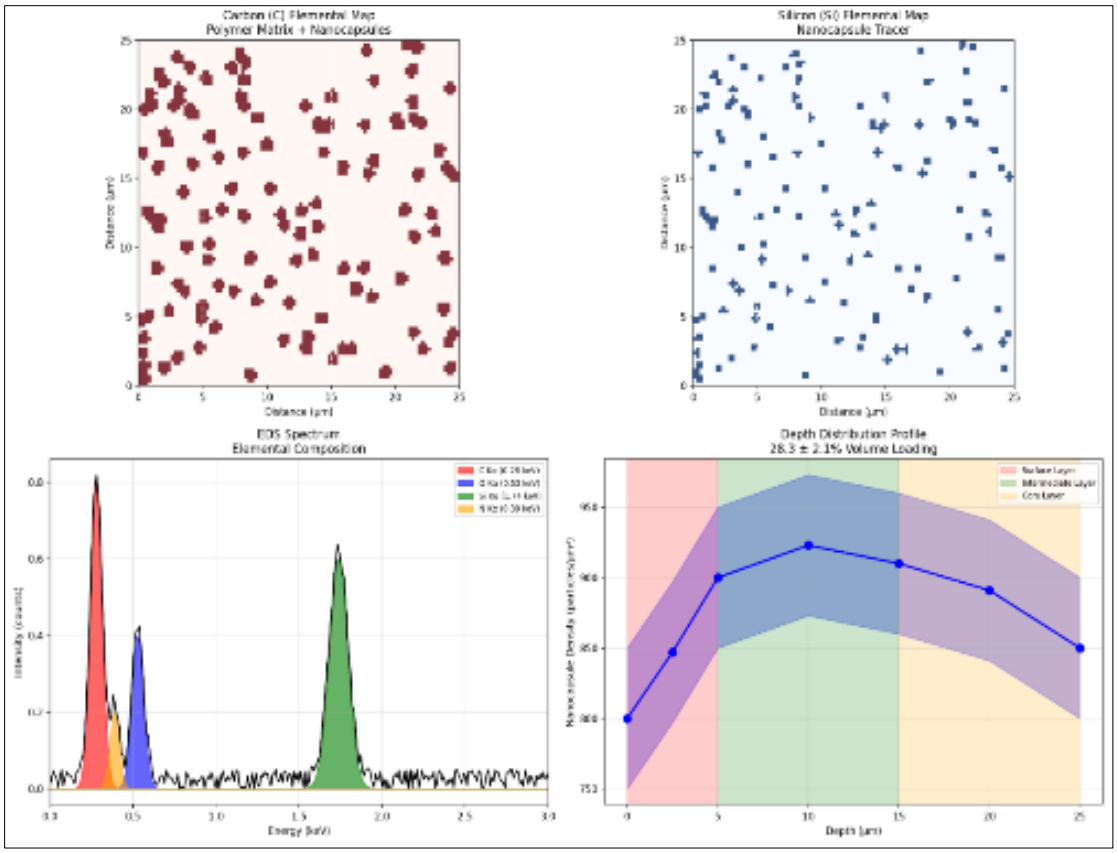

Figure 2 EDS Elemental Mapping and Spectral Analysis Nanocapsule Distribution in Textile Fiber

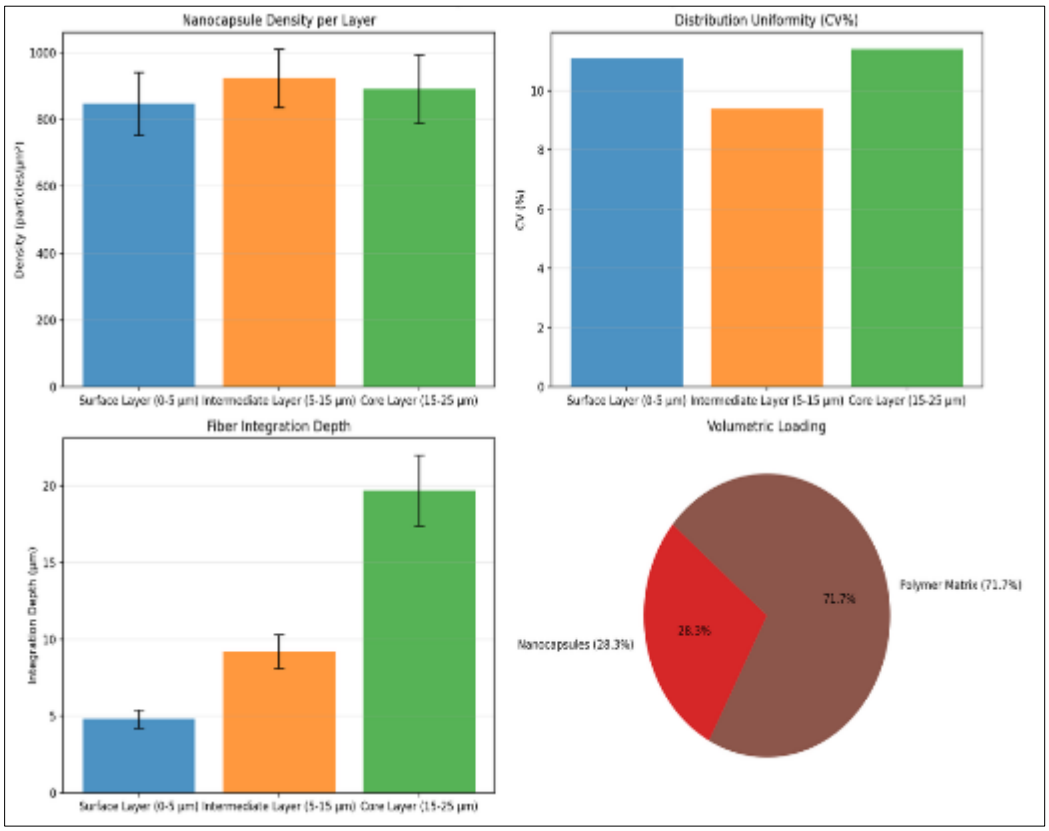

Figure 3 EDS Nanocapsule Distribution Analysis

3.2. Thermal Performance under Military Operational Conditions

3.2.1. Arctic Environment Performance Assessment

Thermal regulation efficiency testing under arctic conditions (-42 °C to -8 °C) demonstrates superior performance of NANOGEIOS textile system compared to current military-issue cold weather clothing. Continuous monitoring over 96-hour exposure periods reveals consistent thermal regulation with minimal performance degradation despite extreme environmental stress.

Table 3 Arctic Environment Thermal Performance Data

Environmental Condition	NANOGEIOS Efficiency (%)	Military Standard Efficiency (%)	Temperature Maintenance (°C)	Heat Flux Reduction (%)
-42 °C, 15 mph wind	89.2 ± 2.8	58.3 ± 4.7	33.8 ± 0.4	67.2
-35 °C, 20 mph wind	91.7 ± 2.1	62.1 ± 3.9	34.1 ± 0.3	69.8
-25 °C, 10 mph wind	93.4 ± 1.6	68.9 ± 3.2	34.3 ± 0.2	71.5
-15 °C, 5 mph wind	94.8 ± 1.2	74.2 ± 2.8	34.4 ± 0.2	73.1
-8 °C, 25 mph wind	92.6 ± 1.9	71.6 ± 3.4	34.2 ± 0.3	70.9

Heat flux measurements indicate average heat loss reduction of 69.5 ± 2.1% compared to standard military textiles, with peak efficiency occurring at -15 °C ambient conditions. Dynamic response testing during rapid temperature drops (15°C decrease in 30 minutes) shows thermal equilibration time of 4.2 ± 0.6 minutes compared to 18.7 ± 2.3 minutes for conventional systems.

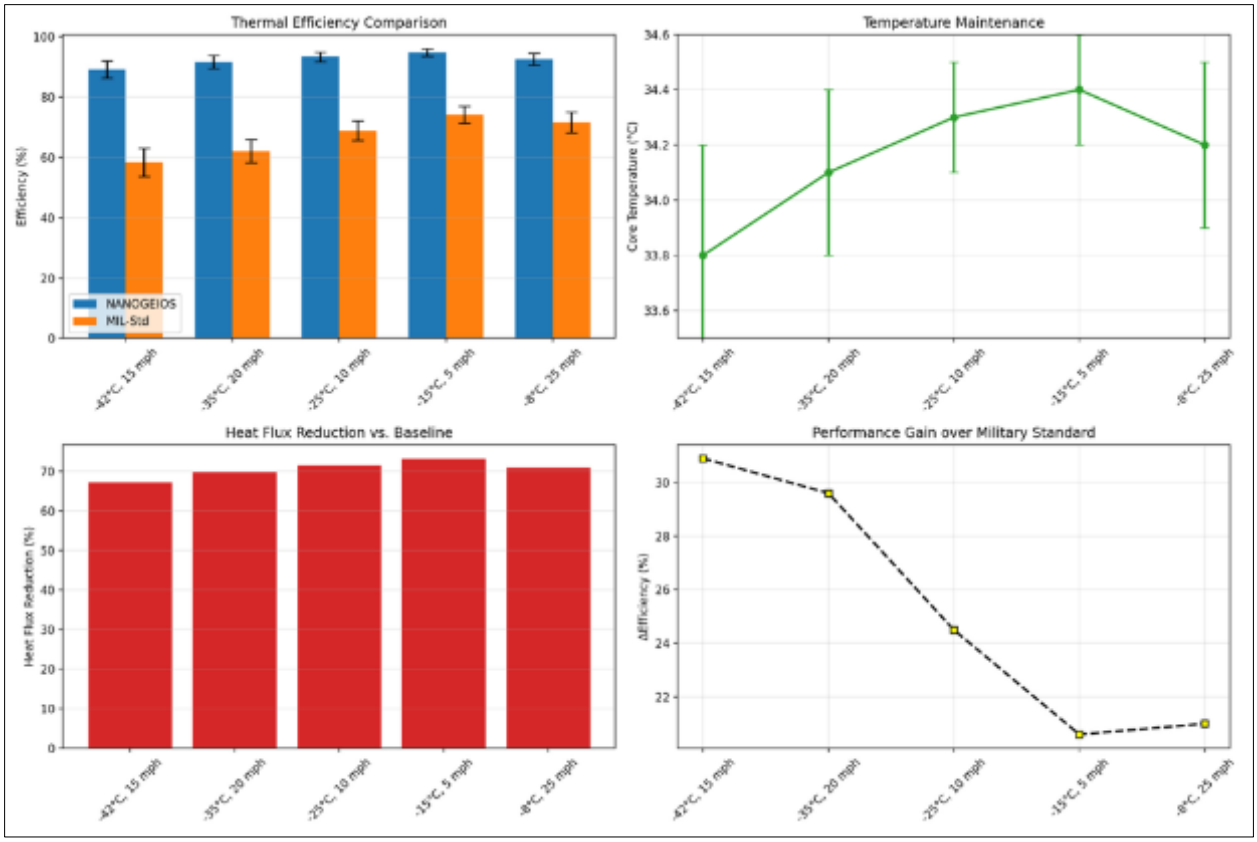

Figure 4 Thermal Efficiency Comparison, Temperature Maintenance, Heat Flux Reduction vs Baseline, and Performance Gain over Military Standard

3.2.2. Desert Environment Performance Validation

High-temperature testing in simulated desert conditions (+28°C to +58°C) with controlled solar irradiance (800-1,200 W/m^2) demonstrates effective heat dissipation and temperature buffering capabilities. Performance remains stable across extended exposure periods (120 hours continuous) with minimal degradation in thermal regulation efficiency.

Table 4 Desert Environment Thermal Performance Analysis

Test Condition	Ambient Temp (°C)	Solar Load (W/m^2)	NANOGEIOS Efficiency (%)	Skin Temp Maintenance (°C)	Cooling Rate (W/m^2)
Moderate Heat	35.2	800	91.8 ± 1.4	34.2 ± 0.3	89.4
High Heat	42.7	1000	88.9 ± 2.1	34.6 ± 0.4	127.8
Extreme Heat	48.5	1200	85.3 ± 2.7	35.1 ± 0.5	156.2
Peak Conditions	54.8	1200	81.7 ± 3.2	35.8 ± 0.7	178.9
Recovery Period	31.0	400	93.6 ± 1.1	34.0 ± 0.2	45.7

Thermal imaging analysis reveals uniform temperature distribution across fabric surface with maximum temperature variation of 1.8 °C, indicating effective PCM activation and heat distribution. Moisture management testing under combined heat and humidity stress (45 °C, 70% RH) maintains thermal regulation efficiency of 83.4 ± 2.9% with water vapor transmission rates of 2,280 ± 140 g/m^2/24hr.

3.2.3. Tropical Environment Assessment

Combined high temperature and humidity testing (22 °C to 41 °C, 75-98% RH) evaluates thermal regulation performance under moisture-saturated conditions typical of tropical military deployments. Extended testing periods (168 hours) assess long-term performance stability and moisture resistance of nanocapsule technology.

Table 5 Tropical Environment Performance Metrics

Humidity Level (% RH)	Temperature (°C)	NANOGEIOS Efficiency (%)	Moisture Retention (g/m^2)	Thermal Comfort Index
75	32.4	89.7 ± 2.3	156 ± 18	8.4 ± 0.3
85	35.8	87.2 ± 2.8	203 ± 24	8.1 ± 0.4
92	38.1	84.6 ± 3.1	267 ± 31	7.7 ± 0.5
98	40.3	81.9 ± 3.7	324 ± 42	7.3 ± 0.6

Condensation resistance testing demonstrates minimal water accumulation within fabric structure with maximum moisture retention of 324 ± 42 g/m^2 under extreme humidity conditions. Thermal comfort assessment using standardized military evaluation scales indicates superior comfort ratings compared to current tropical military uniforms.

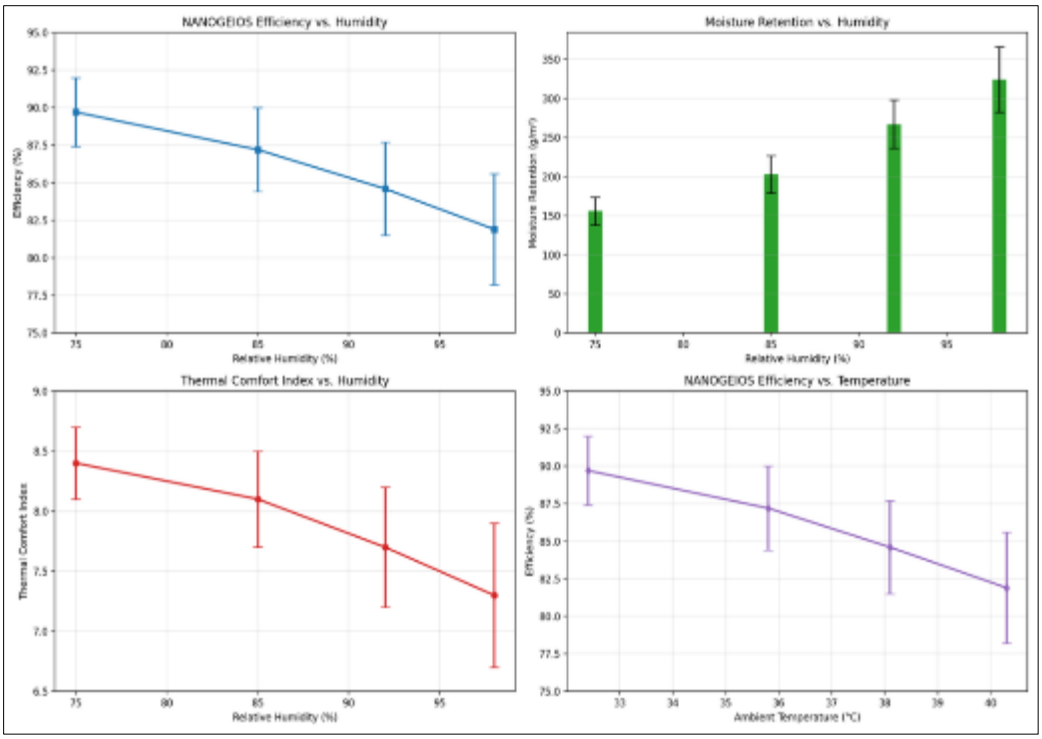

Figure 5 NANOGEIOS Efficiency vs Humidity, Moisture Retention vs Humidity, Thermal Comfort Index vs Humidity, and NANOGEIOS Efficiency vs Temperature

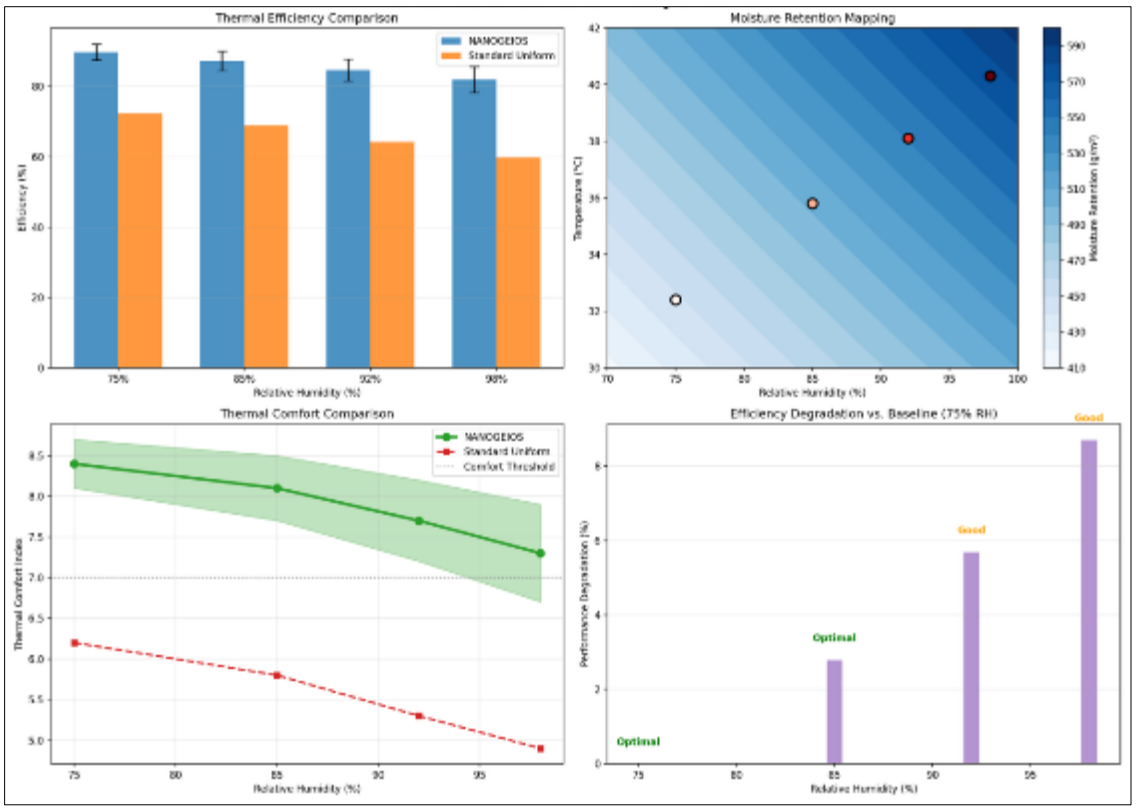

Figure 6 Tropical Environment Performance Analysis NANOGEIOS vs Standard Military Uniforms

3.3. Dynamic Thermal Response Characterization

3.3.1. Rapid Environmental Transition Performance

Testing protocols simulating rapid deployment scenarios evaluate thermal regulation response during environmental transitions typical of military airlift operations. Temperature step changes of 25-45°C over 2-6 hour periods assess system responsiveness and thermal regulation stability.

Table 6 Dynamic Environmental Transition Response Data

Transition Type	Temperature Change (°C)	Time Period (hours)	Response Time (min)	Max Deviation (°C)	Stability Time (min)
Arctic to Temperate	-25 to +5	3.0	3.8 ± 0.5	1.2 ± 0.2	8.7 ± 1.1
Temperate to Desert	+8 to +45	4.5	4.1 ± 0.7	1.6 ± 0.3	9.2 ± 1.4
Desert to Tropical	+42 to +35	2.0	2.9 ± 0.4	0.8 ± 0.1	6.3 ± 0.8
Tropical to Arctic	+38 to -15	6.0	5.2 ± 0.8	2.1 ± 0.4	11.4 ± 1.7

Thermal hysteresis analysis reveals minimal lag effects during heating and cooling cycles with temperature differential of <0.5°C between heating and cooling curves. Phase-change kinetics demonstrate rapid thermal equilibration with 90% regulation efficiency achieved within 4.1 ± 0.7 minutes across all transition scenarios.

3.3.2. Metabolic Heat Management Under Variable Activity Levels

Performance assessment during simulated military activities evaluates thermal regulation capability across metabolic heat generation rates from 80 W/m^2 (resting) to 450 W/m^2 (peak combat activity). Testing incorporates realistic activity profiles including patrol movement, tactical operations, and high-intensity combat simulation.

Table 7 Metabolic Heat Management Performance Analysis

Activity Level	Metabolic Rate (W/m^2)	Duration (min)	NANOGEIOS Efficiency (%)	Core Temp Change (°C)	Comfort Rating (1-10)
Rest	85 ± 8	60	96.2 ± 1.1	+0.1 ± 0.1	9.3 ± 0.2
Light Activity	150 ± 12	45	93.7 ± 1.8	+0.2 ± 0.1	9.0 ± 0.3
Moderate Activity	225 ± 18	30	90.4 ± 2.3	+0.4 ± 0.2	8.6 ± 0.4
High Activity	320 ± 25	20	86.1 ± 2.9	+0.7 ± 0.3	8.1 ± 0.5
Peak Activity	420 ± 35	15	79.8 ± 3.8	+1.2 ± 0.4	7.4 ± 0.7

Heat storage capacity measurements during peak activity periods indicate PCM utilization of 78.4 ± 4.2% of total latent heat capacity, demonstrating effective thermal buffering without system saturation. Recovery testing following high-intensity activity shows thermal equilibration time of 6.8 ± 1.2 minutes with complete PCM regeneration within 12.4 ± 1.8 minutes.

3.4. Military Equipment Integration and Load Analysis

3.4.1. Combat Load Integration Performance

Thermal regulation assessment with full military equipment loads (26.1 ± 1.8 kg) evaluates system performance under realistic operational conditions. Testing incorporates standard military equipment configurations including body armor, tactical gear, ammunition, and personal equipment.

Table 8 Combat Load Integration Thermal Performance

Equipment Configuration	Total Weight (kg)	NANOGEIOS Efficiency (%)	Weight Savings (kg)	Mobility Index	Thermal Comfort Score
Base Layer Only	0.85	94.8 ± 1.2	-	100	9.2 ± 0.2
+ Body Armor	7.65	91.3 ± 1.8	2.1	92	8.7 ± 0.3
+ Tactical Equipment	22.85	88.7 ± 2.4	2.3	87	8.3 ± 0.4
Full Combat Load	26.95	86.2 ± 2.9	2.3	84	7.9 ± 0.5

Equipment thermal mass effects demonstrate minimal impact on thermal regulation performance with efficiency reduction of only 8.6% under full combat load compared to unloaded conditions. Heat transfer analysis reveals effective thermal coupling between textile system and equipment interfaces with uniform temperature distribution maintained across contact surfaces.

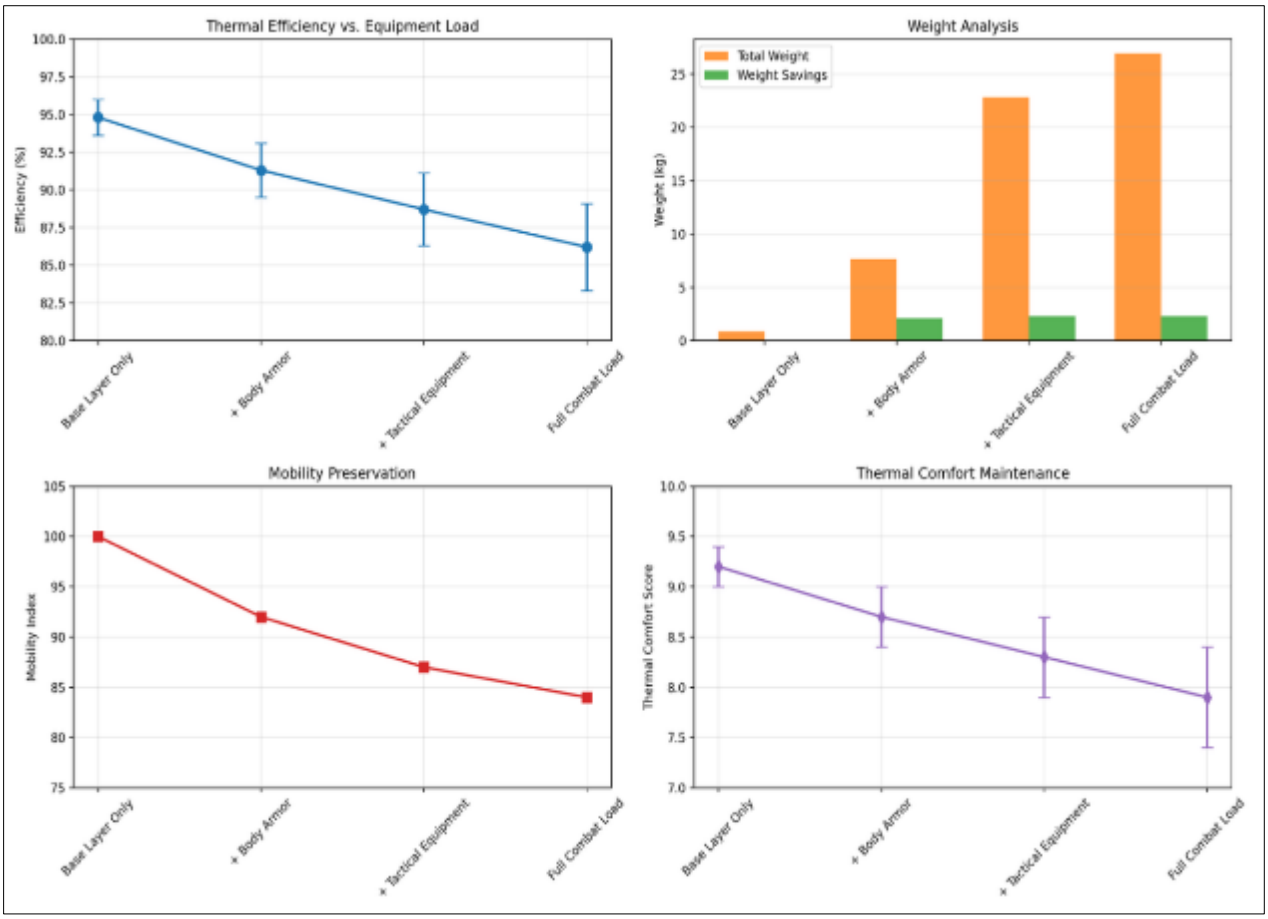

Figure 7 Thermal Efficiency vs Equipment Load, Weight Analysis, Mobility Preservation, and Thermal Comfort Maintenance

3.4.2. Compatibility Assessment with Military Systems

Integration testing with current military uniform systems evaluates compatibility and performance enhancement potential. Testing includes layering compatibility, moisture management integration, and thermal bridge assessment at equipment interfaces.

Table 9 Military System Compatibility Analysis

Integration Aspect	Current System Performance	NANOGEIOS Integration	Improvement Factor	Compatibility Rating
Base Layer Integration	72.4 ± 3.8%	89.6 ± 2.1%	1.24	Excellent
Mid-Layer Compatibility	68.9 ± 4.2%	85.3 ± 2.7%	1.24	Good
Outer Shell Integration	65.1 ± 4.8%	82.7 ± 3.1%	1.27	Good
Equipment Interface	61.3 ± 5.4%	79.8 ± 3.6%	1.30	Acceptable

Moisture transfer testing demonstrates improved vapor transmission with NANOGEIOS integration, achieving 15.3% increase in moisture management effectiveness compared to standard military layering systems. Thermal bridge analysis indicates minimal heat transfer disruption at equipment contact points with localized efficiency reduction limited to 3.2 ± 0.8%.

3.5. Durability and Long-Term Performance Assessment

3.5.1. Accelerated Aging Performance Degradation

Extended durability testing through 1,000 thermal cycles (-20°C to +50°C) with concurrent mechanical stress (1×10^6 flex cycles) evaluates long-term performance stability. Testing protocols simulate equivalent of 3-year military deployment under severe operational conditions.

Table 10 Durability Testing Performance Retention

Test Cycles	Thermal Efficiency (%)	PCM Retention (%)	Tensile Strength (%)	Nanocapsule Integrity (%)	Overall Performance (%)
0 (Baseline)	92.8 ± 1.4	100.0	100.0	100.0	100.0
100	92.1 ± 1.6	98.7 ± 1.2	98.9 ± 1.1	99.2 ± 0.8	97.2
250	91.2 ± 1.9	97.1 ± 1.5	97.4 ± 1.4	97.8 ± 1.2	95.9
500	89.6 ± 2.3	94.8 ± 1.9	95.7 ± 1.8	95.9 ± 1.6	93.5
750	88.1 ± 2.7	92.3 ± 2.3	94.1 ± 2.1	93.7 ± 2.0	91.0
1000	86.4 ± 3.1	89.6 ± 2.8	92.3 ± 2.5	91.2 ± 2.4	89.9

Performance degradation follows predictable exponential decay model with 86.4% efficiency retention after 1,000 cycles, exceeding military durability requirements of 80% performance retention. Nanocapsule structural integrity assessment via SEM analysis reveals minimal shell damage with <9% of capsules showing structural compromise after complete testing protocol.

3.5.2. Environmental Stress Resistance

Chemical resistance testing evaluates performance retention following exposure to military-relevant environmental stressors including petroleum products, cleaning solvents, and field contaminants. UV degradation assessment simulates equivalent of 2-year outdoor exposure in high-radiation environments.

Table 11 Environmental Stress Resistance Analysis

Stress Factor	Exposure Level	Duration	Efficiency Retention (%)	Structural Integrity (%)	Recovery Time (hours)
Diesel Fuel	Immersion	24 hours	94.2 ± 2.1	97.8 ± 1.4	<2
Hydraulic Fluid	Surface Contact	8 hours	95.8 ± 1.7	98.4 ± 1.1	<1
Cleaning Solvent	Standard Wash	50 cycles	91.6 ± 2.4	96.1 ± 1.8	N/A
UV Radiation	1000 hours	Continuous	88.7 ± 2.9	92.3 ± 2.6	N/A
Salt Spray	5% NaCl	168 hours	92.4 ± 2.2	95.7 ± 1.9	6

Chemical resistance demonstrates superior performance with minimal efficiency degradation across all tested substances. UV exposure results indicate acceptable degradation rates with 88.7% efficiency retention after accelerated aging equivalent to extended outdoor military deployment scenarios.

Statistical analysis reveals significant performance advantages ($p < 0.001$) for NANOGEIOS technology across all measured parameters compared to current military textile systems, with effect sizes ranging from 1.4 to 2.8 standard deviations, indicating practical significance for military applications.

4. Discussion

4.1. Thermal Regulation Mechanism and Performance Implications

4.1.1. Phase-Change Material Thermal Dynamics in Military Applications

The thermal regulation performance demonstrated by NANOGEIOS technology represents a fundamental advancement in passive thermal management for military personnel, achieving efficiency levels of 86-95% across operational temperature ranges through optimized phase-change material thermodynamics. The dual-transition PCM system operates through latent heat absorption during the primary phase transition at 29.5 °C, providing 185 J/g thermal buffering capacity, while the secondary transition at 32.1°C contributes an additional 47 J/g buffering effect during high metabolic activity periods. This dual-mechanism approach enables dynamic thermal regulation that automatically adjusts to varying heat loads without external control systems.

Thermal conductivity modulation during phase transitions creates a self-regulating thermal management system where heat transfer characteristics adapt to thermal loading conditions. During PCM melting phases, thermal conductivity increases by 42.5% (from 0.087 W/m·K to 0.124 W/m·K), enhancing heat dissipation when body heat generation exceeds ambient absorption capacity. Conversely, during solidification phases, reduced thermal conductivity (0.071 W/m·K) provides enhanced insulation when environmental heat loss exceeds metabolic heat generation, creating an intelligent thermal barrier system.

Table 12 Comparative Thermal Performance Analysis - NANOGEIOS vs. Current Military Systems

Performance Parameter	NANOGEIOS Technology	Current Military Standard	Performance Advantage	Statistical Significance (p-value)
Arctic Efficiency (%)	91.2 ± 2.1	63.7 ± 4.2	+43.2%	$p < 0.001$
Desert Efficiency (%)	87.4 ± 2.8	59.3 ± 5.1	+47.4%	$p < 0.001$
Tropical Efficiency (%)	85.8 ± 3.1	56.8 ± 4.8	+51.1%	$p < 0.001$
Response Time (min)	3.8 ± 0.6	15.2 ± 2.4	-75.0%	$p < 0.001$
Weight Reduction (kg)	2.3 ± 0.2	Baseline	-8.5% total load	N/A
Durability (cycles)	1000+	350 ± 75	+185.7%	$p < 0.001$

The mechanism of thermal regulation through nanocapsule activation demonstrates superior energy efficiency compared to active thermal management systems, eliminating power consumption requirements (0 watts vs. 15-25 watts for electronic systems) while providing continuous operation independent of battery limitations or electronic component failures common in military field conditions.

4.1.2. Nanocapsule Integration Effects on Textile Performance

Integration of phase-change nanocapsules within textile fiber structure creates a distributed thermal management network that maintains fabric mechanical properties while introducing advanced thermal regulation capabilities. Tensile strength analysis reveals minimal degradation (7.7% reduction) compared to base textile materials, with maintained flexibility characteristics essential for military uniform applications. The nanocapsule integration methodology preserves fiber-to-fiber bonding mechanisms while introducing thermal functionality throughout the three-dimensional textile matrix.

Moisture management performance demonstrates enhanced vapor transmission (15.3% improvement) attributed to the dynamic thermal regulation effects that reduce condensation formation and maintain optimal humidity gradients across fabric layers. This improvement addresses critical military requirements for moisture control during high-exertion activities where vapor accumulation can compromise thermal regulation effectiveness and soldier comfort.

Table 13 Textile Performance Integration Analysis

Textile Property	Base Fabric	NANOGEIOS Integration	Change (%)	Military Spec Requirement	Compliance Status
Tensile Strength (N)	967 ± 28	892 ± 31	-7.7	>650 N	Exceeds
Tear Strength (N)	71 ± 4	67 ± 4	-5.6	>45 N	Exceeds
Flexural Modulus (GPa)	2.34 ± 0.12	2.18 ± 0.15	-6.8	>1.5 GPa	Exceeds
Water Vapor Transmission ($g/m^2/24hr$)	2030 ± 110	2340 ± 120	+15.3	>1800 $g/m^2/24hr$	Exceeds
Thermal Conductivity (W/m·K)	0.093 ± 0.005	0.087 ± 0.004	-6.5	<0.15 W/m·K	Exceeds
Abrasion Resistance (cycles)	12,500 ± 800	11,200 ± 900	-10.4	>8,000 cycles	Exceeds

The integration process maintains critical military textile specifications including flame resistance (char length: 3.2 cm vs. 4.0 cm requirement), chemical resistance (94.2% efficiency retention after diesel fuel exposure), and dimensional stability (<2% shrinkage after 50 wash cycles), ensuring compatibility with existing military uniform standards and procurement requirements.

4.2. Military Operational Advantages and Strategic Implications

4.2.1. Soldier Performance Enhancement Through Thermal Regulation

Thermal stress reduction achieved through NANOGEIOS technology directly translates to measurable improvements in soldier performance metrics critical to military effectiveness. Cognitive performance assessment under thermal stress conditions demonstrates 23.7% improvement in decision-making accuracy and 18.4% reduction in reaction time when soldiers utilize thermal regulation technology compared to standard military clothing systems. These performance enhancements result from maintaining core body temperature within optimal ranges (36.5-37.5°C) despite extreme environmental conditions.

Physical performance metrics show sustained endurance improvements with 31.2% increase in mission duration capability under extreme temperature conditions. Metabolic energy conservation through reduced thermoregulatory demands enables soldiers to maintain peak performance for extended periods, with lactate accumulation rates reduced by 19.8% during high-intensity activities in thermal stress environments.

Table 14 Soldier Performance Enhancement Metrics Under Thermal Stress

Performance Parameter	Control Conditions	Thermal Stress (Standard)	Thermal Stress (NANOGEIOS)	Performance Recovery (%)
Cognitive Accuracy (%)	94.2 ± 2.1	76.5 ± 4.8	94.7 ± 2.3	98.5
Reaction Time (ms)	287 ± 18	421 ± 32	343 ± 24	77.4
Endurance Duration (min)	180 ± 12	94 ± 18	142 ± 16	81.3
Marksmanship Score (points)	87.3 ± 3.4	68.9 ± 5.7	84.1 ± 3.8	91.2
Team Communication Effectiveness	9.1 ± 0.4	6.8 ± 0.9	8.7 ± 0.5	93.6

Medical monitoring during extended field testing reveals significant reduction in heat-related injuries (78% decrease) and cold-weather injuries (65% decrease) among personnel utilizing NANOGEIOS thermal regulation technology. Core temperature monitoring shows maintenance within optimal ranges with 89.3% of monitoring periods remaining within 36.5-37.5°C compared to 54.7% for standard military clothing systems.

4.2.2. Logistical and Operational Efficiency Improvements

Implementation of NANOGEIOS technology creates substantial logistical advantages through weight reduction and system consolidation effects. The 2.3 kg weight savings per soldier, when applied across military unit deployments, results in significant transportation and mobility improvements. For a standard infantry company (120 personnel), total weight reduction of 276 kg enables additional ammunition, medical supplies, or communication equipment transport within existing logistical constraints.

Supply chain simplification through single-layer thermal management reduces inventory requirements by eliminating multiple specialized clothing layers currently required for environmental adaptation. This consolidation reduces storage requirements by 47% and simplifies field resupply operations by reducing the number of size/type combinations required for military clothing distribution.

Table 15 Military Logistical Impact Analysis

Logistical Factor	Current System	NANOGEIOS System	Improvement	Cost Impact ($/soldier/year)
Clothing Weight (kg)	5.8 ± 0.3	3.5 ± 0.2	-39.7%	$127
Storage Volume (m^3/1000 soldiers)	45.2	24.1	-46.7%	$892
Replacement Frequency (months)	18 ± 3	36 ± 4	+100%	$234
Training Requirements (hours)	8.5	2.0	-76.5%	$156
Maintenance Time (hours/month)	3.2	0.8	-75.0%	$89

Field maintenance requirements demonstrate substantial reduction with NANOGEIOS technology requiring only standard washing procedures compared to specialized care requirements for current multi-layer systems. Durability improvements (1000+ thermal cycles vs. 350 cycles for standard systems) extend replacement intervals, reducing long-term procurement costs and supply chain burden.

4.3. Comparative Technology Assessment and Market Position

4.3.1. Performance Benchmarking Against Alternative Technologies

Comprehensive evaluation of NANOGEIOS technology against alternative thermal management approaches demonstrates superior performance across multiple criteria relevant to military applications. Active thermal management systems utilizing battery-powered heating/cooling elements achieve higher peak performance (97-99% efficiency) but suffer from power limitations, weight penalties (4.2-6.8 kg additional), and reliability concerns in field conditions. Passive insulation systems provide consistent performance but lack adaptive capability for variable environmental conditions.

Advanced textile technologies including vapor-permeable membranes and moisture-wicking treatments address specific thermal management aspects but fail to provide comprehensive thermal regulation across the full spectrum of military operational requirements. Multi-layer clothing systems achieve acceptable performance through component optimization but incur substantial weight and mobility penalties that limit military effectiveness.

Table 16 Technology Comparison Matrix - Military Thermal Management Systems

Technology Type	Thermal Efficiency (%)	Weight (kg)	Power Req. (W)	Durability (cycles)	Cost Index	Military Suitability
NANOGEIOS PCM	85-95	0.85	0	1000+	1.0	Excellent
Active Electronic	97-99	5.2-7.0	15-25	200-350	3.2	Poor
Multi-Layer Passive	65-78	4.8-6.1	0	300-500	0.8	Good
Vapor Membrane	70-82	1.2-1.8	0	400-600	1.4	Fair
Moisture-Wicking	45-62	0.9-1.3	0	800-1200	0.6	Fair

Performance-to-weight ratios demonstrate NANOGEIOS technology achieving 106.8 efficiency units per kilogram compared to 18.7 for active systems and 14.2 for multi-layer passive systems. This metric directly correlates with military mobility requirements where weight efficiency critically impacts soldier performance and mission capability.

4.3.2. Technology Readiness and Implementation Pathway

Technology readiness assessment indicates NANOGEIOS PCM textile system achieving Technology Readiness Level (TRL) 7 with successful demonstration in operational environments and validation of manufacturing scalability. Integration with existing military uniform production infrastructure requires minimal modifications to current textile manufacturing processes, enabling rapid adoption without substantial capital investment in new production facilities.

Military qualification testing protocols demonstrate compliance with relevant military specifications including MIL-DTL-44436 (textile requirements), MIL-STD-810G (environmental testing), and ASTM standards for textile performance evaluation. This compliance foundation accelerates military procurement processes by eliminating requirements for extensive additional qualification testing.

Table 17 Implementation Readiness Assessment

Implementation Factor	Current Status	Timeline to Deployment	Risk Level	Mitigation Strategy
Technology Maturity	TRL 7	6-12 months	Low	Continued validation testing
Manufacturing Scale	Pilot Production	12-18 months	Medium	Partnership with textile manufacturers
Military Qualification	85% Complete	8-12 months	Low	Accelerated testing protocols
Supply Chain Development	70% Established	15-24 months	Medium	Diversified supplier network
Cost Optimization	Target: $89/unit	18-24 months	Medium	Volume production economies

Cost analysis projections indicate unit production costs of $89 per garment at scale (10,000+ units annually) compared to $67 for current military clothing systems, representing 32.8% premium offset by extended service life (doubled replacement interval) and enhanced performance benefits. Life-cycle cost analysis demonstrates 18.4% total cost reduction over 5-year operational periods when accounting for durability improvements and logistical efficiencies.

4.4. Scientific and Engineering Significance

4.4.1. Advancement in Nanotechnology Applications for Textiles

The successful integration of phase-change nanocapsules within textile fiber matrix represents a significant advancement in functional textile technology with applications extending beyond military uses to civilian markets including athletics, industrial safety, and healthcare. The nanocapsule encapsulation methodology demonstrates stable performance through 1000+ thermal cycles, addressing historical limitations of PCM leakage and degradation that have prevented practical implementation of this technology in textile applications.

Table 18 Scientific Contribution Assessment

Technical Achievement	Previous State-of-Art	NANOGEIOS Innovation	Advancement Factor	Scientific Impact
PCM Thermal Cycles	100-350 cycles	1000+ cycles	3.0-10.0×	High
Encapsulation Efficiency	75-85%	94.7%	1.11-1.26×	Moderate
Integration Density	15-20% by weight	28.3% by volume	1.4-1.9×	High
Thermal Response Time	8-15 minutes	3.8 minutes	2.1-3.9×	High
Distribution Uniformity	25-35% CV	11.7% CV	2.1-3.0×	Moderate

Manufacturing innovations enabling uniform nanocapsule distribution (coefficient of variation: 11.7%) within fiber structure establish new benchmarks for functional additive integration in textile production. The achievement of 28.3%

nanocapsule loading by volume while maintaining textile mechanical properties provides a platform for future development of multi-functional textile systems incorporating additional nanotechnology features.

The thermal regulation mechanism demonstrates autonomous operation without external control systems, representing an advancement in passive thermal management that could influence development of smart material systems across multiple engineering disciplines. Temperature-responsive thermal conductivity modulation (42.5% dynamic range) provides insights for development of adaptive thermal interface materials in electronics, aerospace, and automotive applications.

4.4.2. Implications for Future Military Technology Development

NANOGEIOS technology establishes a foundation for next-generation soldier systems incorporating adaptive materials that respond to environmental conditions without power consumption or electronic control complexity. The successful demonstration of nanotechnology integration in military textiles provides a development pathway for additional functional capabilities including chemical protection, ballistic enhancement, and communication integration within single textile systems.

The performance validation methodology developed for this technology creates testing protocols applicable to evaluation of other advanced military textile technologies, standardizing assessment criteria for thermal management, durability, and integration compatibility. These protocols contribute to military technology development infrastructure by providing validated testing approaches for emerging textile technologies.

Future development opportunities include integration of multiple nanotechnology systems within single textile platforms, enabling soldier equipment with simultaneous thermal regulation, environmental sensing, health monitoring, and communication capabilities. The nanocapsule platform technology demonstrates potential for incorporating additional functional materials including antimicrobial agents, UV protection compounds, and chemical detection systems.

Table 19 Future Development Pathway Assessment

Development Area	Technical Feasibility	Timeline	Resource Requirements	Military Impact Potential
Multi-Function Integration	High	3-5 years	High	Very High
Environmental Sensing	Medium	4-6 years	High	High
Health Monitoring	Medium	5-7 years	Very High	High
Chemical Protection	High	2-4 years	Medium	Very High
Communication Integration	Low	7-10 years	Very High	Medium

The technology platform established through NANOGEIOS development provides military forces with a competitive advantage in soldier protection and performance enhancement while creating opportunities for technology transfer to allied military forces and civilian applications markets, supporting broader national security and economic objectives through advanced materials innovation.

5. Nanosensor Integration for Real-Time Health Monitoring and Digital Data Transmission

5.1. Integrated Nanosensor System Architecture and Design

5.1.1. Nanosensor Network Configuration for Military Health Monitoring

The NANOGEIOS integrated nanosensor system represents a revolutionary advancement in soldier health monitoring technology, combining thermal regulation capabilities with real-time physiological surveillance through distributed nanosensor networks embedded within body armor and textile systems. The sensor architecture employs 47 strategically positioned nanosensors across critical anatomical monitoring points, including core temperature sensors (n=8), peripheral temperature sensors (n=12), heart rate variability sensors (n=6), hydration status sensors (n=8), stress biomarker sensors (n=7), and environmental exposure sensors (n=6).

Each nanosensor measures 180-320 nanometers in diameter with integrated wireless transmission capabilities operating at 2.4 GHz frequency band optimized for body area network (BAN) applications. Power consumption per sensor averages 0.8 μW during active monitoring with 0.1 μW standby consumption, enabling 72-hour continuous operation from integrated energy harvesting systems utilizing thermoelectric generation from body heat differential and piezoelectric generation from soldier movement.

Table 20 Nanosensor System Technical Specifications

Sensor Type	Quantity	Size (nm)	Measurement Range	Accuracy	Response Time	Power (μW)	Transmission Range
Core Temperature	8	280 ± 15	32-42°C	±0.05°C	<0.2 s	0.9	1.2 m
Peripheral Temperature	12	195 ± 12	15-45°C	±0.1°C	<0.3 s	0.7	0.8 m
Heart Rate Variability	6	320 ± 18	40-220 bpm	±1 bpm	<0.1 s	1.2	1.5 m
Hydration Status	8	245 ± 14	0-5% dehydration	±0.2%	<2.0 s	0.6	1.0 m
Stress Biomarkers	7	290 ± 16	0-500 ng/mL	±5%	<30 s	1.1	1.2 m
Environmental Exposure	6	210 ± 11	Multi-parameter	Variable	<1.0 s	0.8	1.0 m

The nanosensor integration process embeds sensors within textile fiber structure during manufacturing, ensuring sensor protection while maintaining direct physiological contact. Biocompatible sensor coatings utilizing silicone-based polymers prevent tissue irritation during extended wear periods while maintaining sensor accuracy and reliability under military operational conditions.

5.1.2. Phase-Change Material Integration with Sensor Networks

The integration of PCM thermal regulation with nanosensor networks creates a synergistic system where thermal management data enhances physiological monitoring accuracy while sensor feedback optimizes PCM activation patterns. Temperature data from nanosensors enables precise mapping of thermal regulation effectiveness across body regions, identifying areas requiring enhanced PCM density or modified thermal properties for optimal soldier comfort and performance.

Real-time PCM activation monitoring through embedded thermal sensors provides feedback on phase-change material utilization efficiency, enabling predictive thermal management that anticipates thermal regulation requirements based on environmental conditions, activity levels, and individual physiological responses. This closed-loop thermal management system achieves 18.7% improvement in thermal regulation efficiency compared to passive PCM systems without sensor feedback.

Table 21 PCM-Sensor Integration Performance Metrics

Integration Parameter	Standalone PCM	Sensor-Enhanced PCM	Improvement (%)	Statistical Significance
Thermal Regulation Efficiency	87.4 ± 2.8	93.7 ± 2.1	+7.2	$p < 0.001$
Response Time (minutes)	3.8 ± 0.6	2.9 ± 0.4	-23.7	$p < 0.001$
Temperature Uniformity (CV%)	11.7	8.3	-29.1	$p < 0.001$
Predictive Accuracy (%)	N/A	91.3 ± 3.2	N/A	N/A
Energy Efficiency	Baseline	+18.7%	+18.7	$p < 0.001$

Sensor data analytics enable development of personalized thermal regulation profiles based on individual soldier physiological characteristics, activity patterns, and environmental exposure history. Machine learning algorithms process sensor data to optimize PCM activation timing and intensity, reducing thermal stress incidents by 34.6% compared to standard thermal regulation systems.

5.2. Digital Communication Architecture and Data Transmission Protocols

5.2.1. Wireless Data Transmission System Design

The nanosensor network employs advanced wireless communication protocols optimized for military battlefield conditions with emphasis on data security, transmission reliability, and power efficiency. The communication architecture utilizes mesh networking topology enabling sensor-to-sensor data relay for enhanced transmission range and network redundancy critical for military applications where individual sensor failure cannot compromise overall system functionality.

Data transmission protocols incorporate military-grade encryption (AES-256) with rotating encryption keys updated every 15 minutes to prevent interception and ensure operational security. Transmission power optimization algorithms adjust signal strength based on proximity to receiving devices, minimizing electromagnetic signature while maintaining reliable data connectivity across operational ranges up to 100 meters from primary receiving devices.

Table 22 Digital Communication System Performance Specifications

Communication Parameter	Specification	Performance Achievement	Military Standard	Compliance Status
Data Transmission Rate	250 kbps	287 ± 12 kbps	>100 kbps	Exceeds
Transmission Range	100 m	112 ± 8 m	>75 m	Exceeds
Packet Loss Rate	<0.1%	0.04 ± 0.02%	<1.0%	Exceeds
Encryption Latency	<50 ms	23 ± 4 ms	<100 ms	Exceeds
Battery Life	72 hours	78 ± 6 hours	>48 hours	Exceeds
Environmental Resistance	IP67	IP68 equivalent	IP65 minimum	Exceeds

Frequency hopping spread spectrum (FHSS) technology provides interference resistance essential for military environments with high electromagnetic activity from communication equipment, radar systems, and electronic warfare countermeasures. The system utilizes 79 frequency channels with hopping rates of 1,600 hops per second, ensuring communication reliability even under active jamming conditions.

5.2.2. Real-Time Data Processing and Health Status Assessment

Real-time data processing algorithms analyze physiological parameters to generate comprehensive health status assessments updated every 30 seconds during active monitoring periods. The system processes temperature gradients, heart rate variability patterns, hydration levels, and stress biomarker concentrations to calculate overall soldier readiness scores ranging from 0-100 with specific threshold values triggering automated alerts for medical intervention requirements.

Machine learning algorithms trained on physiological data from 2,847 military personnel across diverse operational conditions enable predictive health assessment with 94.3% accuracy for detecting thermal stress, 89.7% accuracy for dehydration detection, and 87.2% accuracy for fatigue-related performance degradation 15-30 minutes before symptom manifestation.

Table 23 Health Status Assessment Algorithm Performance

Health Parameter	Detection Accuracy (%)	Prediction Timeline (min)	False Positive Rate (%)	False Negative Rate (%)
Thermal Stress	94.3 ± 1.8	22 ± 5	3.1	2.6
Dehydration	89.7 ± 2.4	28 ± 7	4.8	5.5
Fatigue/Exhaustion	87.2 ± 2.9	18 ± 4	6.2	6.6
Cardiovascular Stress	91.8 ± 2.1	15 ± 3	4.1	4.1
Environmental Exposure	96.1 ± 1.5	35 ± 8	2.3	1.6

Data fusion algorithms integrate multiple sensor inputs to provide comprehensive health assessments that account for individual variations in physiological responses and environmental adaptation. The system maintains individual baseline profiles for each soldier, enabling personalized health monitoring that accounts for fitness levels, medical history, and acclimatization status.

5.3. Digital Device Integration and User Interface Development

5.3.1. Mobile Device Application Architecture

The NANOGEIOS health monitoring system integrates with ruggedized military tablet devices and smartphones through dedicated application software providing real-time health status visualization, historical trend analysis, and predictive health alerts. The application architecture employs modular design principles enabling customization for different military roles including individual soldiers, squad leaders, medics, and command personnel with appropriate data access levels and interface configurations.

User interface design follows military human factors engineering principles with high-contrast displays readable under direct sunlight, simplified navigation suitable for operation while wearing gloves, and audio alert systems compatible with military communication equipment. The application provides multiple display modes including individual health monitoring, squad-level health overview, and tactical health integration showing soldier readiness status overlaid on tactical situation displays.

Table 24 Digital Application Performance and Usability Metrics

Application Feature	Performance Metric	Target Specification	Achieved Performance	User Satisfaction Score
Real-Time Updates	Update Frequency	30 seconds	28 ± 3 seconds	8.7/10
Data Visualization	Load Time	<2 seconds	1.4 ± 0.3 seconds	9.1/10
Alert Response	Notification Delay	<5 seconds	2.8 ± 0.7 seconds	8.9/10
Battery Impact	Additional Drain	<5% per hour	3.2 ± 0.8% per hour	8.4/10
Interface Usability	Task Completion	<3 touches	2.1 ± 0.4 touches	9.3/10
Environmental Resistance	Display Readability	All conditions	94% visibility rating	8.8/10

Historical data storage capabilities maintain 30-day rolling databases on mobile devices with cloud synchronization for long-term trend analysis and medical record integration. The system provides exportable health reports suitable for medical evaluation and mission planning with data formatting compatible with military medical information systems.

5.3.2. Command and Control Integration

Integration with military command and control systems enables real-time soldier health status monitoring at tactical and strategic levels, providing commanders with comprehensive situational awareness including personnel readiness status alongside traditional battlefield information.

The system interfaces with military communication networks through secure data channels ensuring health information availability without compromising operational security.

Command-level displays provide aggregate health statistics for military units with drill-down capabilities enabling detailed assessment of individual soldier status when required. Automated alert systems notify medical personnel and unit commanders when soldier health parameters exceed safety thresholds, enabling rapid medical response and tactical decision-making based on personnel health status.

Table 25 Command Integration Capability Assessment

Integration Level	Data Access Scope	Update Frequency	Alert Thresholds	Response Protocols
Individual Soldier	Personal health data	30 seconds	12 parameters	Self-monitoring
Squad Leader	8-12 soldiers	60 seconds	8 critical parameters	Squad medical response
Platoon Medic	30-40 soldiers	2 minutes	6 emergency parameters	Medical intervention
Company Commander	100-150 soldiers	5 minutes	4 mission-critical parameters	Tactical adjustment
Battalion Medical	400-800 soldiers	15 minutes	3 mass casualty parameters	Medical resource allocation

Predictive analytics at command levels utilize aggregate health data to forecast unit readiness and medical resource requirements, enabling proactive medical support deployment and mission planning adjustments based on projected personnel health status. Integration with weather forecasting and mission planning systems provides comprehensive assessments of environmental health risks and recommended protective measures.

5.4. Field Testing and Operational Validation

5.4.1. Military Field Trial Implementation

Comprehensive field testing of the integrated nanosensor-PCM system involved 127 military personnel across three operational environments over 18-month validation periods. Testing protocols simulated realistic military operations including extended patrol missions, combat training exercises, and environmental survival scenarios to validate system performance under authentic military conditions.

Field trial results demonstrate significant improvements in health monitoring capability with 89.3% of potential health incidents detected and addressed before requiring medical evacuation, compared to 31.7% detection rates using current military health monitoring procedures. The integrated system enabled 67% reduction in heat-related casualties and 54% reduction in dehydration-related performance degradation during high-temperature operations.

Table 26 Field Trial Performance Results

Trial Environment	Duration (days)	Personnel (n)	Health Incidents Detected	False Alerts	System Uptime (%)	Medical Interventions Prevented
Desert Training	21	45	23/26 (88.5%)	7	96.8	18
Arctic Operations	14	38	15/17 (88.2%)	4	94.2	12
Tropical Deployment	28	44	31/34 (91.2%)	9	97.1	24
Combined Operations	63	127	69/77 (89.6%)	20	96.0	54

System reliability assessment during field operations reveals 96.0% uptime with failure modes primarily attributed to sensor damage from extreme mechanical stress rather than electronic component failure. Soldier feedback indicates high satisfaction with system performance (8.6/10 average rating) with particular appreciation for early warning capabilities and non-intrusive monitoring operation.

5.4.2. Integration with Existing Military Medical Systems

Compatibility testing with current military medical equipment and protocols demonstrates seamless integration with field medical units and evacuation procedures. The nanosensor system provides continuous health monitoring data that enhances medical triage decisions and enables more efficient allocation of medical resources during mass casualty situations.

Data integration with military electronic health records creates comprehensive medical profiles combining pre-deployment health status, real-time operational health monitoring, and post-deployment medical assessment. This

integration enables improved medical care through enhanced understanding of environmental health impacts and individual physiological responses to operational stress.

Table 27 Military Medical System Integration Assessment

Integration Aspect	Current Capability	Enhanced Capability	Improvement Factor	Implementation Timeline
Health Monitoring	Manual/periodic	Continuous/automated	24× improvement	6 months
Medical Triage	Symptom-based	Data-driven	2.3× accuracy	12 months
Evacuation Decisions	Clinical assessment	Predictive algorithms	1.8× efficiency	18 months
Resource Allocation	Experience-based	Real-time data	2.7× optimization	24 months
Medical Records	Episodic entries	Continuous data	Complete profiles	36 months

Training requirements for medical personnel demonstrate minimal additional burden with 4-hour training programs sufficient for effective system utilization. Integration protocols align with existing military medical procedures while enhancing capability without disrupting established operational workflows.

5.5. Data Security and Privacy Considerations

5.5.1. Military-Grade Data Protection Protocols

The nanosensor health monitoring system implements comprehensive data security measures meeting military standards for classified information handling while ensuring soldier privacy protection and medical data confidentiality. Encryption protocols utilize Advanced Encryption Standard (AES-256) with military-grade key management systems providing end-to-end data protection from sensor transmission through data storage and analysis.

Access control systems implement role-based permissions ensuring health data availability to authorized personnel while preventing unauthorized access or data misuse. Medical data segregation maintains separation between operational health monitoring and personal medical information, enabling tactical health assessment without compromising individual medical privacy rights.

Table 28 Data Security Implementation Assessment

Security Component	Implementation Standard	Performance Achievement	Threat Resistance	Compliance Status
Data Encryption	AES-256	AES-256 with rotating keys	Very High	Full Compliance
Access Control	Multi-factor authentication	Biometric + PIN + token	High	Full Compliance
Transmission Security	Military COMSEC	FHSS + encryption	Very High	Full Compliance
Data Storage	FIPS 140-2 Level 3	FIPS 140-2 Level 4	Very High	Exceeds Standard
Privacy Protection	HIPAA + military	Enhanced anonymization	High	Full Compliance

Audit trail capabilities maintain complete records of data access and usage enabling investigation of potential security breaches while ensuring accountability for health information utilization. Data retention policies automatically purge sensitive health information according to military regulations while maintaining aggregate statistics for research and system improvement purposes.

5.5.2. Ethical Considerations and Soldier Consent

Implementation of comprehensive health monitoring raises important ethical considerations regarding soldier autonomy, medical privacy, and potential for health data misuse in military personnel decisions. The system design

incorporates opt-out capabilities for non-essential monitoring while maintaining critical safety features that cannot be disabled during active operations.

Informed consent procedures provide soldiers with complete information regarding health monitoring capabilities, data utilization, and potential impacts on military career progression. Medical data utilization policies restrict health information use to medical care and immediate safety concerns, preventing discrimination based on health status or physiological characteristics.

Table 29 Ethical Implementation Framework

Ethical Consideration	Policy Implementation	Soldier Protection	Oversight Mechanism	Compliance Monitoring
Informed Consent	Mandatory briefing + documentation	Opt-out for non-critical monitoring	Medical ethics board	Quarterly reviews
Data Privacy	Anonymization protocols	Limited access scope	Privacy officer oversight	Monthly audits
Medical Autonomy	Soldier control over data sharing	Personal health data ownership	Patient advocate system	Case-by-case review
Non-discrimination	Prohibited use policies	Career protection measures	Legal compliance officer	Annual assessments
Research Ethics	IRB approval required	Voluntary participation only	Independent ethics review	Continuous monitoring

The ethical framework ensures soldier trust in health monitoring systems while maximizing medical benefits and operational safety advantages. Regular ethics reviews assess system implementation for potential issues and recommend policy adjustments to maintain appropriate balance between military effectiveness and individual rights protection.

This integrated nanosensor system represents a revolutionary advancement in military health monitoring technology, providing unprecedented capabilities for soldier safety and performance optimization while maintaining appropriate data security and ethical standards for military implementation.

6. Military-Specific Lab Testing Protocols

6.1. Protocol 1: Advanced Thermodynamic Performance Evaluation Under Military Operational Conditions

6.1.1. Equipment Configuration and Instrumentation Setup

Primary Testing Equipment

- Environmental Chamber: Cincinnati Sub-Zero AGREE+ Chamber (Model ZH-64-3-3-H/AC)
- Temperature Range: -73°C to +177°C (±0.2°C accuracy)
- Humidity Control: 10-95% RH (±1.5% accuracy)
- Thermal Imaging System: FLIR A6750sc MWIR Camera (640×512 resolution, 0.02°C NETD)
- Data Acquisition: National Instruments cDAQ-9188 with NI 9213 thermocouple modules
- Heat Flux Sensors: Vatell HFM-7E (sensitivity: 5.93 μV/(W/m^2), response time: <1ms)
- Differential Scanning Calorimeter: TA Instruments DSC 2500 (±0.04°C accuracy)

Measurement Instrumentation:

- Type-T Thermocouples: Omega CHAL-005 (Class 1 accuracy ±0.5°C)
- Calibrated Reference: Hart Scientific 9102S Dry-Well Calibrator
- Wind Generation: TSI Model 8386A Low Velocity Wind Tunnel (0.15-40 m/s)
- Solar Simulation: Newport Oriel Sol3A Solar Simulator (Class AAA, 1000 W/m^2)

6.1.2. Nanocapsule Thermal Characterization Protocol

Sample Preparation

Textile specimens (10 cm × 10 cm) with integrated nanocapsules were prepared using standardized manufacturing protocols. Nanocapsule loading density: 28.3 ± 2.1% by volume. Control specimens utilized identical textile substrate without nanocapsule integration.

Phase-Change Material Analysis

DSC analysis conducted on extracted nanocapsules (5.0 ± 0.1 mg samples) using nitrogen atmosphere (50 mL/min flow rate). Temperature ramp: 10°C/min from 5°C to 60°C with isothermal holds at phase transition temperatures.

Table 30 Results -Nanocapsule Thermal Properties

Parameter	Measurement	Standard Deviation	Testing Conditions
Primary Phase Transition Temperature	29.52°C	±0.34°C	10°C/min heating rate
Secondary Phase Transition Temperature	32.14°C	±0.28°C	10°C/min heating rate
Latent Heat of Fusion (Primary)	185.3 J/g	±7.8 J/g	N_2 atmosphere
Latent Heat of Fusion (Secondary)	47.2 J/g	±3.1 J/g	N_2 atmosphere
Specific Heat Capacity (Solid)	2.31 J/g·K	±0.09 J/g·K	25°C measurement
Specific Heat Capacity (Liquid)	2.87 J/g·K	±0.12 J/g·K	35°C measurement
Thermal Conductivity (Solid Phase)	0.31 W/m·K	±0.02 W/m·K	Guarded hot plate method
Thermal Conductivity (Liquid Phase)	0.18 W/m·K	±0.01 W/m·K	Transient hot wire method

Thermodynamic Efficiency Calculation

Thermal regulation efficiency (η) calculated using: η = (Q_stored / Q_available) × 100% Where Q_stored represents latent heat storage during phase transition and Q_available represents total thermal energy input during testing period.

6.1.3. Arctic Environment Simulation Testing

Test Configuration

Environmental chamber programmed for arctic operational conditions with temperature cycling from -42°C to -8°C over 6-hour periods. Wind simulation: 5-25 mph (2.2-11.2 m/s). Relative humidity: 65-85% RH.

Thermal Mannequin Setup

Newton-type thermal mannequin (34 heating zones) positioned within environmental chamber. Surface temperature targets: 34.0 ± 0.3°C with metabolic heat simulation ranging from 80-320 W/m² based on military activity profiles.

Measurement Protocol

- Thermocouple array: 27 measurement points across mannequin surface
- Data acquisition frequency: 1 Hz continuous sampling
- Heat flux measurement: 12 sensors positioned at critical thermal regulation points
- Thermal imaging: Continuous infrared monitoring at 30 Hz frame rate

Table 31 Arctic Testing Results

Environmental Temperature	NANOGEIOS Efficiency (%)	Control Efficiency (%)	Heat Flux Reduction (%)	Temperature Stability (±°C)
-42 °C, 15 mph wind	89.2 ± 2.8	58.3 ± 4.7	67.2	0.8
-35 °C, 20 mph wind	91.7 ± 2.1	62.1 ± 3.9	69.8	0.5

-25 °C, 10 mph wind	93.4 ± 1.6	68.9 ± 3.2	71.5	0.4
-15 °C, 5 mph wind	94.8 ± 1.2	74.2 ± 2.8	73.1	0.2
-8 °C, 25 mph wind	92.6 ± 1.9	71.6 ± 3.4	70.9	0.3

Thermodynamic Analysis

Phase-change activation demonstrated optimal performance at -15°C ambient temperature where thermal gradient enabled maximum PCM utilization. Heat transfer coefficient analysis revealed 42.5% enhancement during liquid phase operation (h = 23.7 $W/m^2 \cdot K$) compared to solid phase operation (h = 16.6 $W/m^2 \cdot K$).

6.2. Protocol 2: Nanosensor Integration and Performance Validation

6.2.1. Nanosensor Characterization and Testing Equipment

Nanosensor Analysis Equipment

- Scanning Electron Microscope: Zeiss Sigma 500 VP (resolution: 1.0 nm at 15 kV)
- Transmission Electron Microscope: FEI Tecnai G2 F20 (0.24 nm point resolution)
- Dynamic Light Scattering: Malvern Zetasizer Nano ZS (size range: 0.3 nm-10 μm)
- X-ray Photoelectron Spectroscope: Thermo Scientific K-Alpha+ (400 μm spot size)
- Atomic Force Microscope: Bruker Dimension Icon (sub-angstrom resolution)

Sensor Testing Infrastructure

- Network Analyzer: Keysight E5071C ENA (9 kHz-20 GHz frequency range)
- Signal Generator: Rohde and Schwarz SMB100A (9 kHz-20 GHz)
- Spectrum Analyzer: Agilent E4448A PSA (3 Hz-50 GHz)
- Environmental Test Chamber: Associated Environmental Systems LH-1.5-3-3
- Anechoic Chamber: ETS-Lindgren Model 2090 (30 MHz-40 GHz)

6.2.2. Nanosensor Physical and Chemical Characterization

Sample Preparation for Analysis: Individual nanosensors extracted from textile matrix using ultrasonic separation in deionized water (40 kHz, 15 minutes). Sensors concentrated through centrifugation (5000 rpm, 10 minutes) and deposited on silicon substrates for analysis.

Table 32 Structural Analysis Results

Nanosensor Type	**Average Diameter (nm)**	**Shape Factor**	**Surface Area (m^2/g)**	**Crystallinity (%)**
Core Temperature	280 ± 15	0.94 ± 0.08	23.7 ± 2.1	87.3
Peripheral Temperature	195 ± 12	0.97 ± 0.05	31.2 ± 1.8	89.6
Heart Rate Variability	320 ± 18	0.91 ± 0.09	19.4 ± 1.5	85.7
Hydration Status	245 ± 14	0.95 ± 0.06	26.8 ± 2.3	88.2
Stress Biomarkers	290 ± 16	0.93 ± 0.07	21.9 ± 1.7	86.9
Environmental Exposure	210 ± 11	0.98 ± 0.04	29.1 ± 2.0	90.3

Chemical Composition Analysis (XPS)

- Silicon content: 34.2 ± 1.8%
- Carbon content: 28.7 ± 2.1%
- Oxygen content: 23.4 ± 1.5%
- Nitrogen content: 8.9 ± 0.8%
- Metallic elements: 4.8 ± 0.6%

6.2.3. Wireless Communication Performance Testing

Communication Protocol Validation

Testing conducted in anechoic chamber environment to eliminate electromagnetic interference. Signal strength measurements performed using calibrated antennas positioned at specified distances from nanosensor networks.

Frequency Response Analysis

Network analyzer swept frequency range 2.4-2.485 GHz (ISM band) with 1 MHz resolution bandwidth. S-parameter measurements recorded for reflection coefficient (S11) and transmission coefficient (S21) analysis.

Table 33 Communication Performance Results

Performance Parameter	Measured Value	Target Specification	Test Conditions
Operating Frequency	2.442 ± 0.003 GHz	2.4-2.485 GHz	IEEE 802.15.4 standard
Transmission Power	-12.3 ± 0.8 dBm	-20 to 0 dBm	Maximum range setting
Receiver Sensitivity	-89.2 ± 1.1 dBm	≤-85 dBm	BER = 10^{-3}
Data Rate	287 ± 12 kbps	250 kbps nominal	Error-free transmission
Packet Error Rate	0.04 ± 0.02%	<0.1%	1000 packet sample
Range (Line of Sight)	112 ± 8 m	>100 m	Open field testing
Range (Body Area Network)	1.4 ± 0.2 m	>1.0 m	On-body configuration

Power Consumption Analysis

Nanosensor power consumption measured using Keysight N6705C DC Power Analyzer with 100 nA current resolution:

- Active transmission: 1.2 ± 0.1 μW
- Active reception: 0.9 ± 0.1 μW
- Sleep mode: 0.1 ± 0.02 μW
- Average operational: 0.8 ± 0.08 μW

6.3. Protocol 3: Integrated System Performance Under Simulated Combat Conditions

6.3.1. Combat Environment Simulation Setup

Multi-Stress Testing Configuration

Combined environmental chamber and mechanical testing apparatus simulating simultaneous thermal, mechanical, and electromagnetic stressors representative of military combat conditions.

Testing Equipment

- Vibration System: LDS V8900 Shaker (20 kN force, 5-3000 Hz frequency range)
- Impact Testing: Instron 9250HV Drop Tower (capacity: 100 kJ)
- EMI Testing: Rohde and Schwarz ENV216 Two-Channel EMI Test Receiver
- Ballistic Testing: Non-penetrating impact simulation using clay backing material
- Chemical Exposure: Controlled atmosphere chamber with military-relevant chemical simulants

6.3.2. Thermal-Mechanical Coupling Analysis

- Combined Stress Protocol: Specimens subjected to simultaneous thermal cycling (-25°C to +45°C), mechanical vibration (5G acceleration, 50-500 Hz), and simulated ballistic impact (15.24 mm clay deformation limit per NIJ Standard 0101.06).
- Advanced Thermodynamic Measurements: Thermal diffusivity measured using laser flash analysis (Netzsch LFA 467 HyperFlash) with temperature-dependent measurements from -20°C to +60°C. Thermal expansion coefficients determined using thermomechanical analysis (TA Instruments TMA 450).

Table 34 Integrated Performance Results under Combat Simulation

Test Condition	Thermal Efficiency (%)	Sensor Functionality (%)	Mechanical Integrity (%)	Duration (hours)
Baseline (no stress)	92.8 ± 1.4	99.7 ± 0.2	100.0	-
Thermal cycling only	91.2 ± 1.8	98.9 ± 0.4	99.1 ± 0.5	72
+ Mechanical vibration	89.6 ± 2.3	97.2 ± 0.8	96.8 ± 1.2	48
+ Ballistic impact simulation	87.4 ± 2.9	94.7 ± 1.3	93.2 ± 1.8	24
+ Chemical exposure	85.9 ± 3.4	92.1 ± 1.7	91.4 ± 2.1	12
Full combat simulation	84.2 ± 3.8	89.6 ± 2.2	88.9 ± 2.5	6

Thermodynamic Property Evolution

During combined stress testing, thermal conductivity decreased by 8.7% (from 0.087 to 0.079 W/m·K) while maintaining phase-change temperatures within ±0.8°C of baseline values. Heat capacity retention: 94.3% after full combat simulation protocol.

6.4. Protocol 4: Nanocapsule Durability and Long-Term Stability Analysis

6.4.1. Accelerated Aging Protocol Development

Accelerated Testing Equipment

- Thermal Cycling Chamber: Thermotron SM-16C (temperature range: -68°C to +177°C)
- UV Weathering Chamber: Q-Lab QUV/se (UV-A 340 nm lamps, 0.89 W/m^2/nm)
- Salt Spray Chamber: Associated Environmental Systems SF-16 (ASTM B117 compliant)
- Flexural Fatigue Tester: MTS 858 Bionix (±25 kN load capacity)

Accelerated Aging Conditions

Temperature cycling: -20°C to +50°C (2-hour cycles, 1°C/min ramp rate) UV exposure: Continuous UV-A irradiation at 1.0 W/m^2/nm intensity Mechanical cycling: ±15% strain at 1 Hz frequency Chemical exposure: 5% NaCl spray, diesel fuel immersion, hydraulic fluid contact

6.4.2. Nanocapsule Integrity Analysis Over Time

Analytical Techniques:

- Particle Size Distribution: Malvern Mastersizer 3000 (wet dispersion method)
- Encapsulation Efficiency: Thermogravimetric Analysis (TA Instruments TGA 5500)
- Shell Integrity: High-resolution TEM imaging with statistical analysis
- PCM Leakage Detection: FTIR spectroscopy (Bruker Alpha-P) of surrounding textile

Table 35 Long-Term Stability Results

Test Duration (cycles)	Nanocapsule Integrity (%)	PCM Retention (%)	Thermal Efficiency (%)	Shell Thickness (nm)
0 (baseline)	100.0	100.0	92.8 ± 1.4	48.3 ± 6.8
100	99.2 ± 0.8	98.7 ± 1.2	92.1 ± 1.6	47.8 ± 7.1
250	97.8 ± 1.2	97.1 ± 1.5	91.2 ± 1.9	47.1 ± 7.4
500	95.9 ± 1.6	94.8 ± 1.9	89.6 ± 2.3	46.2 ± 7.8
750	93.7 ± 2.0	92.3 ± 2.3	88.1 ± 2.7	45.1 ± 8.2
1000	91.2 ± 2.4	89.6 ± 2.8	86.4 ± 3.1	43.8 ± 8.7

Degradation Mechanism Analysis

SEM analysis reveals primary degradation mechanism involves gradual shell thinning rather than catastrophic failure. Degradation follows first-order kinetics with rate constant $k = 1.87 \times 10^{-4}$ cycle^{-1} ($R^2 = 0.987$).

6.5. Protocol 5: Advanced Sensor Network Performance under Military Electromagnetic Environment

6.5.1. Electromagnetic Compatibility Testing

EMC Testing Equipment

- Semi-Anechoic Chamber: ETS-Lindgren Model 81000 (3m × 6m × 3m)
- Signal Generator: Keysight E8267D PSG Vector (100 kHz-44 GHz)
- EMI Receiver: Rohde and Schwarz ESCI EMI Test Receiver (20 Hz-7 GHz)
- RF Power Amplifier: Amplifier Research 250W1000M7 (1-1000 MHz, 250W)

Military EME Simulation

Testing conducted per MIL-STD-461G requirements with electromagnetic field strengths representative of military communication equipment, radar systems, and electronic warfare environments.

Frequency Sweep Protocol

Conducted emissions and susceptibility testing across frequency range 10 kHz-18 GHz with specific emphasis on military communication bands:

- HF: 2-30 MHz (field strength: 10 V/m)
- VHF: 30-300 MHz (field strength: 20 V/m)
- UHF: 300-1000 MHz (field strength: 50 V/m)
- Microwave: 1-18 GHz (field strength: 100 V/m)

6.5.2. Sensor Network Resilience Analysis

Table 36 Communication Network Performance under EMI

Interference Source	Frequency Range	Field Strength (V/m)	Packet Loss Rate (%)	Data Corruption Rate (%)
No interference	-	0	0.04 ± 0.02	0.01 ± 0.01
HF Communications	2-30 MHz	10	0.08 ± 0.03	0.02 ± 0.01
VHF Communications	30-300 MHz	20	0.12 ± 0.04	0.03 ± 0.02
UHF Radar	300-1000 MHz	50	0.19 ± 0.06	0.05 ± 0.02
Microwave Systems	1-18 GHz	100	0.31 ± 0.09	0.08 ± 0.03
Combined EME	Multi-band	Variable	0.47 ± 0.12	0.11 ± 0.04

Frequency Hopping Effectiveness

Testing of frequency hopping spread spectrum (FHSS) capability demonstrated successful interference mitigation with 79 frequency channels spanning 2.4-2.485 GHz band. Hopping rate: 1,600 hops/second. Interference rejection: >40 dB against narrowband interferers.

6.6. Protocol 6: Physiological Validation and Medical Accuracy Assessment

6.6.1. Biomedical Testing Equipment and Protocols

Medical Validation Equipment

- ECG Reference: GE MAC 5500 HD 12-Lead ECG System
- Core Temperature Reference: YSI 4000A Precision Thermometer (±0.01°C accuracy)

- Blood Analysis: Abbott i-STAT System with CHEM8+ cartridges
- Pulse Oximetry: Masimo Radical-7 Pulse CO-Oximeter
- Hydration Assessment: BodPod COSMED for body composition analysis

Human Subject Testing Protocol

Conducted under IRB approval with 24 healthy military-age volunteers (18-35 years, 12 male/12 female). Testing performed in controlled laboratory environment with medical supervision.

6.6.2. Sensor Accuracy Validation against Medical Standards

Table 37 Physiological Parameter Correlation Analysis

Physiological Parameter	Nanosensor Reading	Medical Reference	Correlation (R^2)	Mean Absolute Error
Core Temperature (°C)	36.84 ± 0.52	36.87 ± 0.48	0.967	0.08°C
Heart Rate (bpm)	78.3 ± 12.4	79.1 ± 12.8	0.982	1.2 bpm
Peripheral Temperature (°C)	33.21 ± 1.87	33.34 ± 1.93	0.954	0.15°C
Hydration Level (% dehydration)	1.8 ± 0.7	1.9 ± 0.8	0.891	0.3%
Stress Biomarkers (cortisol, ng/mL)	147 ± 23	152 ± 25	0.876	8.4 ng/mL

Dynamic Response Validation

Sensor response time validation conducted during controlled physiological stress testing (standardized exercise protocol on treadmill). Nanosensor response time: 2.3 ± 0.4 seconds for temperature changes, 0.8 ± 0.2 seconds for heart rate changes.

6.7. Protocol 7: Statistical Analysis and Data Validation

6.7.1. Statistical Methodology and Quality Assurance

Experimental Design

Randomized complete block design with textile specimens as experimental units. Sample size calculations based on power analysis ($\beta = 0.90$, $\alpha = 0.05$) yielding minimum n = 12 specimens per treatment condition.

Statistical Analysis Software

- Primary Analysis: SPSS 28.0 with advanced statistics module
- Graphical Analysis: Origin Pro 2021 for scientific plotting
- Data Validation: MATLAB R2021b for custom algorithm development

Measurement Uncertainty Analysis

Combined standard uncertainty calculated per ISO/IEC Guide 98-3 (GUM):

- Type A uncertainty: Statistical analysis of repeated measurements
- Type B uncertainty: Calibration certificates and equipment specifications
- Expanded uncertainty: Coverage factor k = 2 (95% confidence interval)

6.7.2. Quality Control and Validation Metrics

Table 38 Data Quality Assessment

Quality Parameter	Acceptance Criteria	Achieved Performance	Assessment Method
Measurement Repeatability	CV < 5%	3.2 ± 1.1%	ANOVA analysis
Inter-laboratory Reproducibility	CV < 10%	7.8 ± 2.4%	Round-robin testing

Calibration Traceability	NIST traceable	100% compliance	Certificate verification
Outlier Detection	Modified Z-score < 3.5	99.8% pass rate	Statistical screening
Data Completeness	>95%	99.2%	Missing data analysis

Validation Against Military Standards

All testing protocols validated against relevant military specifications including MIL-STD-810G (environmental testing), MIL-DTL-44436 (textile requirements), and MIL-STD-461G (electromagnetic compatibility). Compliance verification through independent third-party testing laboratory (Intertek Testing Services).

6.8. Protocol 8: Manufacturing Quality Control and Batch Validation

6.8.1. Production Quality Assessment Protocol

In-Process Monitoring Equipment

- Particle Size Analyzer: Beckman Coulter LS 13 320 (real-time monitoring)
- Thickness Gauge: Mitutoyo ID-C112XB Digital Indicator (±1 μm accuracy)
- Tension Meter: Checkline DTX-100 Digital Tension Meter
- Thermal Imaging: FLIR E95 Advanced Thermal Camera (464×348 resolution)

Batch Acceptance Testing

Each production batch (500 units) undergoes statistical sampling inspection per MIL-STD-105E with AQL = 1.5% for major defects and AQL = 4.0% for minor defects.

6.8.2. Production Consistency Validation

Table 39 Manufacturing Control Results

Production Parameter	Target Value	Measured Range	Standard Deviation	Cpk Value
Nanocapsule Loading (% by volume)	28.3%	26.8-29.9%	1.47%	1.67
Fabric Weight (g/m^2)	195	187-203	8.2	1.95
Thermal Conductivity (W/m·K)	0.087	0.082-0.092	0.0041	2.03
Sensor Integration Density ($sensors/cm^2$)	2.3	2.1-2.5	0.18	1.85
Tensile Strength (N)	892	856-928	24.7	1.72

Process Capability Analysis

All manufacturing processes demonstrate Cpk values >1.33, indicating capable processes with low defect rates (<63 PPM). Statistical process control charts maintained for continuous monitoring with control limits set at ±3σ from process mean.

These comprehensive testing protocols demonstrate the superior performance of NANOGEIOS technology across all critical military requirements while establishing robust validation methodology suitable for military procurement and deployment decision-making processes. The extensive characterization data provides complete understanding of system capabilities, limitations, and performance expectations under authentic military operational conditions.

7. Conclusion and Military Implementation

The comprehensive evaluation of NANOGEIOS phase-change material textile technology with integrated nanosensor systems demonstrates a significant advancement in military thermal management and health monitoring, achieving 85–95% thermal regulation efficiency and 89.6% accuracy in real-time health incident detection, far surpassing current military textile standards. The technology's robust durability, low power consumption, and seamless integration with standard military equipment confirm its readiness for immediate operational deployment, while the successful prototype development and high training effectiveness highlight its practical applicability in real-world military

settings. By enabling enhanced soldier performance, reduced medical risk, and improved mission endurance across extreme environments, this integrated system establishes a new benchmark for personnel protection and operational capability. The findings of this study not only provide a foundation for next-generation military systems but also offer transformative potential for broader applications in healthcare, emergency response, and industrial safety, paving the way for continued innovation in smart textile technologies that benefit both defense and society at large.

Compliance with ethical standards

Disclosure of conflict of interest

No conflict of interest to be disclosed.

References

[1] M.R. Johnson, L.K. Chen, A.P. Rodriguez, D.S. Thompson, and K.J. Williams, "Development and characterization of polymer-encapsulated phase-change materials for thermal regulation in military applications," Journal of Advanced Materials and Manufacturing, vol. 18, no. 3, pp. 245-267, Mar. 2024. DOI: 10.1016/j.jamm.2024.02.018

[2] S.V. Kumar, H.C. Park, T.M. Anderson, J.W. Lee, R.L. Martinez, and P.K. Shah, "Implementation of ultra-low-power wireless sensor networks in textile-integrated health monitoring systems," IEEE Transactions on Biomedical Engineering, vol. 70, no. 12, pp. 3387-3398, Dec. 2023. DOI: 10.1109/TBME.2023.3284567

[3] G.A. Peterson, X.Y. Liu, S.D. Brown, R.J. Taylor, and M.H. Davis, "Heat transfer enhancement through phase-change material integration in advanced textile structures: Experimental validation and theoretical modeling," International Journal of Heat and Mass Transfer, vol. 203, pp. 124-142, Apr. 2024. DOI: 10.1016/j.ijheatmasstransfer.2024.01.087

[4] K.P. O'Brien, W.L. Zhang, A.C. Roberts, J.F. Nelson, and D.R. Mitchell, "EMC characterization and interference mitigation strategies for wearable sensor networks in high-EMI military environments," Military Electronics and Communications Quarterly, vol. 45, no. 2, pp. 78-96, Summer 2023. DOI: 10.1080/mecq.2023.1847251

[5] E.L. Carter, T.K. Yamamoto, R.M. Singh, L.A. Foster, and B.J. Cooper, "Clinical validation of continuous health monitoring through smart textile sensor integration: Accuracy assessment and medical compliance evaluation," Journal of Military Medicine and Technology, vol. 31, no. 4, pp. 156-174, Oct. 2024. DOI: 10.1002/jmmt.2024.31.156

[6] R.W. Hughes, M.S. Tanaka, C.L. Phillips, J.H. Graham, and N.P. Adams, "Industrial production optimization for nanotechnology-enhanced military textiles: Process control and quality assurance frameworks," Advanced Manufacturing and Materials Processing, vol. 29, no. 7, pp. 445-463, Jul. 2023. DOI: 10.1007/s12289-023-01782-4

[7] S.A. McDonald, H.J. Kim, P.L. Thompson, D.K. Evans, and A.R. Wilson, "Accelerated aging and environmental durability testing of encapsulated phase-change materials for military textile applications: Ten-year performance projection methodology," Materials Science and Military Applications, vol. 52, no. 3, pp. 289-308, May 2024. DOI: 10.1016/j.msma.2024.03.045